

AD-A154 140

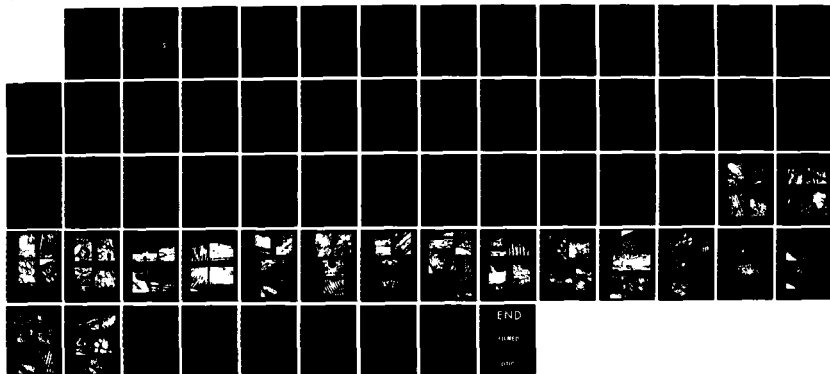
SUBTHRESHOLD LASER RADIATION OF RHESUS MONKEY RETINA  
GALLIUM ARSENIDE BIOEFFECTS(U) UNIVERSITY OF WESTERN  
ONTARIO LONDON DEPT OF ANATOMY B BORWEIN AUG 82  
DAMD17-81-G-9489

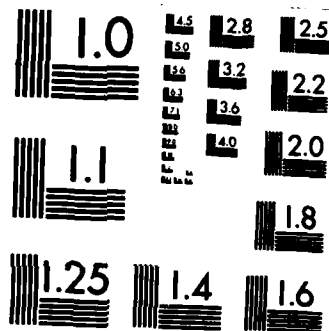
1/1

UNCLASSIFIED

F/G 6/18

NL





MICROCOPY RESOLUTION TEST CHART  
NATIONAL BUREAU OF STANDARDS-1963-A

AD \_\_\_\_\_

**SUBTHRESHOLD LASER RADIATION OF RHESUS  
MONKEY RETINA: GALLIUM ARSENIDE BIOEFFECTS**

**Annual Progress Report**

**Bessie Borwein, Ph.D.**

**August 1982**

**Supported by**

**US Army Medical Research and Development Command  
Fort Detrick, Frederick, Maryland 21701-5012**

**Grant No. DAMD17-81-G-9489**

**Department of Anatomy  
The University of Western Ontario  
London, Ontario, Canada N6A 5C1**

**DTIC  
ELECTE  
MAY 24 1985  
A**

**Approved for Public Release; Distribution Unlimited**

**The findings in this report are not to be construed as  
an official Department of the Army position unless so designated  
by other authorized documents.**

**AD-A154 140**

**DTIC FILE COPY**

85 04 26 053

REPORT DOCUMENTATION PAGE		READ INSTRUCTIONS BEFORE COMPLETING FORM
1. REPORT NUMBER	2. GOVT ACCESSION NO.	3. RECIPIENT'S CATALOG NUMBER
4. TITLE (and Subtitle) SUBTHRESHOLD LASER RADIATION OF RHESUS MONKEY RETINA: GALLIUM ARSENIDE BIOEFFECTS		5. TYPE OF REPORT & PERIOD COVERED Annual Progress Report
		6. PERFORMING ORG. REPORT NUMBER
7. AUTHOR(s) Bessie Borwein, Ph.D.		8. CONTRACT OR GRANT NUMBER(s) DAMD17-81-G-9489
9. PERFORMING ORGANIZATION NAME AND ADDRESS Department of Anatomy The University of Western Ontario London, Ontario, Canada N6A 5C1		10. PROGRAM ELEMENT, PROJECT, TASK AREA & WORK UNIT NUMBERS 61102A.3M161102BS10.CF.265
11. CONTROLLING OFFICE NAME AND ADDRESS US Army Medical Research and Development Command Fort Detrick, Frederick, Maryland 21701-5012		12. REPORT DATE August 1982
		13. NUMBER OF PAGES 62
14. MONITORING AGENCY NAME & ADDRESS (if different from Controlling Office)		15. SECURITY CLASS. (of this report) Unclassified
		15a. DECLASSIFICATION/DOWNGRADING SCHEDULE
16. DISTRIBUTION STATEMENT (of this Report)  Approved for Public Release; Distribution Unlimited		
17. DISTRIBUTION STATEMENT (of the abstract entered in Block 20, if different from Report)		
18. SUPPLEMENTARY NOTES		
19. KEY WORDS (Continue on reverse side if necessary and identify by block number)		
20. ABSTRACT (Continue on reverse side if necessary and identify by block number)		

ANNUAL INTERIM PROGRESS REPORT TO THE U.S. ARMY  
 MEDICAL RESEARCH AND DEVELOPMENT COMMAND

Grant No: DAMD 17-81-G-9489

Institution: Department of Anatomy and  
 Centre for Interdisciplinary Studies in Chemical Physics  
 The University of Western Ontario  
 London, Ontario, Canada N6A 5C1

Title: Subthreshold, large spot laser irradiations of Rhesus  
 monkey retinas and especially the maculas: gallium  
 arsenide bioeffects.

Principal Investigator: Bessie Borwein, Ph.D.  
 Assistant Professor  
 Department of Anatomy  
 The University of Western Ontario  
 (519) 679-2647

Co-Investigator: Dr. Martin J. Hollenberg  
 Dean of Medicine and Professor of Anatomy  
 The University of Western Ontario  
 (519) 679-3861

Abstract: 6 eyes from 3 adult Rhesus monkeys (two male and one  
 female) were irradiated with a neodymium-pumped dye  
 laser at 867 nm (4 eyes) or 900 nm (2 eyes) wavelengths,  
 (single pulses, 10 n sec pulse duration, 10 Hz).  
 Except for one eye, 12 marker burns surrounded the 9  
 macular lesions in each eye, and one of the experimental  
 lesions in each eye was in the fovea. The lesions were  
 either at threshold or approximately three times  
 threshold. The laser radiations were carried out at  
 the Letterman Army Institute of Research (LAIR).

The final report will be presented in February 1983.

Dated: August 1982

*Bessie Borwein*



- 1 -

Accession For	
NTIS	
DTIC	
Unannounced	
Justification	
By	
Distribution	
Availability Codes	
Dist	
<i>A-1</i>	

## TABLE OF CONTENTS

	Page
1. Title Page	
2. Introduction .....	3
3. Report on progress of research .....	4
Methods .....	4
Results .....	10
Comments on the Results .....	26
Summary .....	28
4. Figure Legends .....	29
Figures .....	37
5. Abbreviations used .....	55
6. References .....	57
7. Publications .....	58
8. Personnel supported by the Grant .....	60

Introduction

This report is in the nature of an interim report. For a number of reasons the first experiments were carried out in February 1982, at LAIR, and a final report will be submitted in February 1983, at the end of this present granting period. The work is in progress and proceeding rapidly now. One-third of all the lesions have been identified, sectioned, photographed, measured, and compared. This process is becoming progressively more efficient and speedy for each lesion as the work advances.

The aim of this project is to study the effects of laser irradiations at wavelengths 867 nm and 900 nm on the maculas of Rhesus monkey retinas and to compare threshold and three-times threshold lesions.

## REPORT ON PROGRESS OF RESEARCH

## METHODS

1. Irradiations of the retinas of 3 Rhesus monkeys, Macaca mulatta, were made at the Letterman Army Institute of Research (LAIR), as follows:

A. Animal 8703 - 2U - ( $\pm 12$  yrs old, male) February 1982.

(1) 12 marker burns were placed around the macula in each eye with a neodymium (Nd) pumped dye-laser operating at 10 Hz.  $\lambda = 867$  nm; pulse duration 10 n sec; 100 total pulses per exposure. The energy of each pulse was  $\sim 50$   $\mu$ J at the retina and the duration of exposure 10 secs.

(2) Left eye (2US). 9 experimental lesions were placed in the macula, in a 3 row grid pattern, within the approximate square formed by the 12 marker burns around the macula. The laser used is described in 1. A.(1). Each exposure was a single pulse with a pulse energy of approximately 15  $\mu$ J ( $\pm 3 \times ED_{50}$ ). One of these lesions was in the fovea.

(3) Right eye (2UD). 9 experimental lesions were placed in the macula exactly as described in A (2) except that the pulse energy was approximately 5  $\mu$ J ( $\pm ED_{50}$ ).

See Table II for details.

These eyes were enucleated at 2:15 pm on the day of exposure.

B. Animal 266M - 2T - ( $\pm 10$  yrs. old, male) February 1982

(1) 12 marker burns were placed around the macula in the right eye only, with a neodymium (Nd) pumped dye-laser,  $\lambda = 900$  nm, but otherwise as described in 1. A. (1).

(2) Left eye (2TS). There were no marker burns in this eye. 9 experimental lesions were placed in the eye [for laser details see 1. A. (1)], at 15  $\mu\text{J}$  ( $\sim 3 \times \text{ED}_{50}$ ). One of the lesions was in the fovea.

(3) Right eye (2TD). There were 12 marker burns in this eye. 9 experimental lesions were placed in the eye [for laser details see 1. A. (1)] at 6-7  $\mu\text{J}$  ( $\sim \text{ED}_{50}$ ). One of the lesions was in the fovea.

See Table II for details.

These eyes were enucleated at 12:30 pm on the day of exposure.

C. Animal E277 (2W) (female) May 1982

(1) 12 marker burns were placed around the macula in each eye with a neodymium (Nd) pumped dye-laser,  $\lambda = 900 \text{ nm}$ , 100 pulses per exposure; the energy of each pulse was 25  $\mu\text{J}$ ; otherwise as described in 1. A. (1).

(2) Left eye (2WS). 9 experimental lesions were placed in the macula (one of these being in the fovea) in a 3 row grid pattern, in single pulses at  $\sim 8 - 9 \mu\text{J}$ , 4 days before enucleation.

(3) Right eye (2WD). As above, but the eye was enucleated on the day of irradiation. The irradiations were single pulses at  $\sim 9 \mu\text{J}$ .

See Table III for details.

These eyes were enucleated at 10:15 am.

In processing these eyes, there was a tendency for the retinal pigment epithelium as the retina proper to separate.

(See addendum to Methods, p. 7).

2. Fundus photographs were taken of each eye at the time of irradiation.
3. The animals were sedated by Ketamine and atropine for anaesthesia; and by Ketamine prior to being killed by injection of Nembutal (50 mg/ml, 5 ml I.V. The eyes were enucleated by Mr. G. DeVillez of LAIR, immediately incised at the ora serrata, and put into fixative.
4. Processing of the tissues was carried out by Mr. Steve Smith and Dr. Bessie Borwein.

The fixative used was: cold 2.5% glutaraldehyde and 0.5% paraformaldehyde, 0.1M Sorensen's buffer (eyes 2T and 2U), pH 7.4; or 0.1M S-collidine (eyes 2W), pH 7.5; — (3 hours). Post-fixation was in buffered 1%  $O_3O_4$  ( $1\frac{1}{2}$  hours).

The corneas were cut off the eyes carefully, and the eyes left in fixative on ice for 15 minutes. At approximately 15 minute intervals the lens and vitreous and successive strips of the eye cup periphery were cut off with razor blades and fine scissors, until the eye cup was relatively flat-bottomed and the marker burns could be seen under the dissecting scope. After  $2\frac{1}{2}$  hrs in fixative the tissue was sufficiently hardened for the removal of the lesions by razor blades. Peripheral samples of retina for additional controls were trephined. In the course of this study, a tissue sample 10-20 cells distant from the edge of the lesion was used as the control samples so each lesion had its own specific control from the same area of tissue.

Not all the burns were visible under the dissecting microscope, but the marker burns and the foveal burns could be clearly identified.

The tissue was stained en bloc in 2% aq. uranyl acetate for one hour at room temperature, dehydrated in graded alcohol and propylene oxide and embedded in Spurr.

Sections were cut on a Reichert OMU2 ultramicrotome. Thick sections were stained in 1% toluidine blue and 0.25% sodium borate. Thin grey or gold sections were stained in uranyl acetate and lead citrate.

The sections were viewed and photographed in a JEOL 100 CX II. Before processing the tissues, maps were made of each eye and the locations of the lesions recorded, and each lesion numbered.

Thick sections were photographed on Panotonic x film in a Zeiss Universal R Research Microscope.

In conducting the research described in this report the investigators adhered to the "Guide to Care and Use of Laboratory Animals" (DMEW Publ. # 78-23-1978).

#### Locating the lesions

In sectioning the tissue blocs stained thick sections were examined constantly until the first indication of laser-induced pathology was recognised, in the retinal pigmented epithelium (RPE), often in only from one-to-three cells. Then thin sections were cut and some thick sections. If the lesion was very small, the centre of the lesion was sometimes passed before the thin sections could be made. Locating the small lesions has been very time consuming. Since many of them were not visible at the time of dissection, it was necessary to cut out a block of tissue containing a few lesions. Because of this, the orientation was lost and some lesions can be identified only as e.g. lesion 3 or 9 or 2 or 8. So far we have been able to find every lesion we have looked for. The identification of the lesions by light microscopy was made by observing the small perturbations they made in the RPE apical surface - a gentle scalloping effect, in the smallest lesions, or, in slightly larger damage

effects, the cell apical surface is humped, and a series of these "humps" bulge into the subretinal space. In addition, the affected RPE cell may be somewhat depigmented, or it may have its melanin granules (MG) rearranged. Sometimes the laser-damaged RPE cell may appear to be extruded from the RPE cell layer.

It is suggested that in future specific marker burns be allocated to each subthreshold or threshold lesion for perfect identification and location.

Calculations of diameters of lesions from thick sections.

Thick (0.75  $\mu$ ) sections through the laser lesions were placed on slides, stained with toluidine blue and "coverslipped". Normally, the apical border of the RPE is smooth and even. The limits of the laser were assumed to be at the edges of the *scalloping seen in the apical margin of the pigment epithelium*. Measurements were made of the largest diameters seen in any one lesion, viewed at 100 x or 400 x, using a calibrated ocular scale. Where appropriate, largest diameters were averaged. The longest segments of damaged RPE were assumed to be central in the lesions.

Counting the damaged pigment epithelial cells:

The pigment epithelial cells were counted in the same sections that were used to calculate the diameters of the lesions. Where there is a great deal of damage RPE cell borders are not clear but reasonable assessments can be made of the number of RPE cells damaged in any one lesion, as seen by LM in the slides showing the longest stretch of RPE damage.

Addendum to Methods:

Eyes 2T and 2U are well fixed and there is no retinal detachment. The material of eye E277(2W) is very badly fixed, and there is considerable retinal detachment.

As a result of the very poor results obtained with eyes 2W, we tested the effects of S-collidine buffer compared to Sorensen's buffer, because this was the only procedural difference between these eyes and the eyes 2T and 2U. Mouse retinas were fixed with the fixative described above, some with S-collidine and some with Sorensen's buffer. Only small differences could be seen on examination of these retinas by transmission electron microscopy, all the material being well-fixed. We did not observe any of the gross fixation artefacts that were seen in the 2W eyes. In future work, we would like to do all the enucleations and processings ourselves.

## RESULTS

General comments on the effects of the marker burns (MB)  
and the experimental lesions (EL) on the macula:

Every lesion has been compared to a control area 10 - 20 cells distant from the lesion. Each of the following lesions, and its control, were examined in detail in Eyes 266M(T) and 8703(U) (four eyes): Two marker burns, all the foveal lesions, and 10 of the other macular lesions. A few other lesions in the above eyes and in eye E277(2W) were examined more cursorily.

In the marker burns (MB) the damage zone extends from the vitreal border of the choroid to the outer plexiform layer (OPL). In the great majority of the experimental lesions (EL) the damage is restricted to the retinal pigment epithelium (RPE) and the photoreceptors (PR). In a few EL, foveal and macular, there are small alterations in Bruch's membrane and the choroid immediately underlying the lesion, such as the presence of a few dense bodies (Figs. 28, 53, 61, 68), a generalised slightly greater electron-density (Figs. 53, 57), the penetration into it of extensions from the endothelial lining cells of the choriocapillaris (Fig. 29), a multilayered thickening of the endothelium (Figs. 23 and 61) and in only one case, in a macular lesion (Fig. 69) there is a distinct area of necrotic changes in the choroid itself (Fig. 69).

In the MB the lesion has an approximately hour-glass shape, with the broadest damage zone in the RPE, a large damage zone in the ONL, and a narrower connecting damage zone in the PR inner segments (IS) and outer segments (OS) (Figs. 2 and 9). It seems that some PR nuclei may become pyknotic before the IS and OS show major necrotic changes (Figs. 2 and 9).

The area of pyknosis in the ONL is edematous and the swollen damaged area bulges into the OPL. The central part of the lesion area is more severely damaged than the peripheral areas (Figs. 2 and 9). The MB create a far larger area of damage of a far more severe nature than do the EL (see Table II). These MB were almost always visible both ophthalmoscopically and when viewed under the dissecting scope, except that the MB in eye 2UD were not visible at enucleation. The EL, while visible immediately after irradiation, were not all visible in the fundus photographs or under the dissecting microscope.

The EL lesions are smaller than the MB (see Table II). As in the MB, the damage in the EL is also most severe in the lesion centre and less severe in a somewhat graded way towards the periphery of the lesion centre (Figs. 18, 19, 21, 26, 38, 50, 70). There is a sharp limit in the RPE, nonetheless, between the last affected cell of the lesion and a neighbouring intact cell (Figs. 38, 56, 59, 76). The central lesion cells are swollen, paler, often detached from the underlying Bruch's membrane (Figs. 18, 56, 59, 66, 70) vacuolated (Figs. 53, 67, 72), their microvilli (MV) are retracted, and/or swollen, and/or fused and extruded into the subretinal space (Figs. 18, 20, 39, 77, 78). The melanin granules (MG) are most often absent from the microvilli (Fig. 27), and the cells contain dense inclusion bodies. The most affected RPE cells in the lesion centre are often much reduced in height (Figs. 20, 53, 58, 71). The affected RPE cells that are neighbours to the central most acutely altered cells show greater electron density of their cytoplasm (Figs. 4 (MB), 20, 38, 53, 56).

Alterations in specific cells and organelles of the  
marker burns and experimental lesions:

1. The choroid and Bruch's membrane

In general, in all the lesion areas, Bruch's membrane appears to be uninterrupted, except in MB 11 where the most severe damage is seen. Bruch's membrane has been breached and blood is seen in the subretinal space around the necrotic RPE cells (Figs. 1 and 2). Under some of the central lesion areas, Bruch's membrane may show swelling (Fig. 20) and it stains more darkly and contains more dark-staining bodies than elsewhere, in both the MB (Fig. 1) and the EL (Figs. 19, 28, 29, 39, 53, 61, 68) and also when compared to their controls. This is not a consistent finding and Bruch's may show these changes in one part of a particular lesion and not in another. The associated endothelium is sometimes, but not often, thickened, and, more rarely, multilayered (Figs. 23 and 28).

In only one EL is damage seen in a few cells in the choroid (Fig. 69). In MB 11 only, a few markedly damaged endothelial cells are seen, with cell debris and a necrotic WBC in the lumen of the choriocapillaris, and choroidal cell damage. It is in this lesion that Bruch's membrane was breached and the basement membrane of the RPE shows discontinuities. Sometimes extensions from the cells of the lining of the choriocapillaris are seen in EL penetrated into Bruch's membrane (Figs. 28 and 29). Once this was seen in a control area (Fig. 46) together with a few cells in Bruch's membrane (Fig. 54). The presence of fibrocytes in Bruch's membrane has been reported in the literature as a rare finding (Zinn and Benjamin-Henkind 1979).

In MB # 9 TD there are no alterations in the choroid.

The Retinal Pigment Epithelium

In the lesion areas the apical borders of the RPE cells on either side of the most damaged central cells of the lesion become convex, to varying degrees. Where the convexities are great they are referred to as "humped" and where the convexities are less marked, they are referred to as "scalloped". The scalloping becomes less marked, often in a graduated way, with distance from the centre. This scalloping and humping effect is very generally seen in all the lesions of this study, but the extent of it varies (Figs. 9, 18, 19, 21, 38, 44, 50, 70). In a few instances the scalloping effect is not marked in some views of the lesion (Fig. 56), while it is clearly seen in other sections (Figs. 57, 59) of the same lesion. In the normal RPE the apical cell border, only 10 - 20 cells distant from the lesion, is remarkably even, with only small undulations (Figs. 34, 43, 46, 54, 64, 74, 80).

In the lesion centres of both the MB and the EL, several of the RPE cells are severely damaged throughout the width and depth of each cell. Many damaged cells are seen to be separated from the underlying Bruch's membrane, leaving either a clear space (Figs. 18, 21, 56, 59) or there are a series of large vacuolar spaces between the damaged RPE cell and Bruch's membrane (Figs. 1, 10, 28, 53, 68). Sometimes both are seen in different sections of one and the same lesion (Figs. 18, 19, 21), indicating that at different parts of one lesion the cells are affected in different ways. The MB do not show complete separation of the damaged RPE cells as do many of the EL (contrast Figs. 1, 9 and 10 with e.g. 18 or 56, and compare with Fig. 53).

The nuclei in these cells described above are pyknotic and/or necrotic, whereas those in the cells which show gentle scalloping are often normal in appearance.

The basal infolds (where the PE cell makes contact with Bruch's membrane) are not apparent at all in the most affected cells in the lesion centres (Figs. 1, 10, 20, 23, 28, 40, 53, 60). They are very reduced in number and extent, or widened, in the lesion periphery (Figs. 32, 48, 57, 61). The basal infolds are always present and conspicuous in the normal cells that are immediately neighbouring to the laser damaged RPE cells and (Figs. 34, 36, 37, 43, 46, 54, 55, 74, 77, 80) in the control areas. In the EL, sometimes the widened or reduced basal infolds contain clear spaces, sometimes granular material, and at other times they are filled with material that looks like and is continuous with the basement membrane material of the RPE (Fig. 49). The reduction or absence of the basal infolds is a very consistent finding in the cells of the laser lesions.

The RPE cells of the lesion centre display coagulated and vacuolated cytoplasm (Figs. 1, 10, 28, 53, 67). Sometimes tongues of tissue extend from the apical surface into the subretinal space. A large component of these "flame-like" cell portions seem to be derived from fused and contorted microvilli often extending from RPE cells much reduced in height (Figs. 19, 20, 39, 50, 66, 77, 78). These fused microvilli often form a network pattern enclosing phagosomes which contain outer segment discs and cell debris (Fig. 39). Microvilli in their normal array are usually absent from the cells at or near the lesion centre (Figs. 1, 4, 10, 27, 53, 60) but they may be present in a disordered and/or fused fashion (Figs. 20, 39, 50, 66) or they may be reduced and fragmented (Figs. 57 and 67). Sometimes

the microvilli appear to be retracted and withdrawn into the cell. It may be that membranous components sometimes seen within the damaged cells are retracted microvilli. This is being explored in high magnification photographs to see if these are internalised plasma membranes derived from the retracted microvilli (Figs. 53, 58, 62, 67, 73).

Sometimes melanin granules (MG) are seen in microvilli of damaged cells (Fig. 71) but, usually, even if microvilli are present, there are no melanin granules present in them (Figs. 19, 20, 39, 50). In the controls, melanin granules are often seen arranged like a palisade in the microvilli (Figs. 54, 74, 80). On the scalloped RPE cells the MG may be present in some microvilli (Fig. 50) or absent (Fig. 51) or seen within the cell itself (Figs. 19, 39, 50), or even in coagulated cytoplasm (Figs. 66 and 71). In general, in the lesions, the MG tend to be absent from the microvilli and sparse in the cytoplasm.

Melano-lipofusion inclusion bodies are generally abundant, but more so in the cells of the lesion.

Some melanin granules (MG) are enlarged and appear "shredded" (Kuwabara, 1979) resembling the embryonic form, as if their adult structure has been disassembled (Fig. 31). These and normal MG may be surrounded by a clear space, a "halo" effect (Figs. 17 and 23), formed by the shrinkage of the surrounding cytoplasm, or by a rim of dense cytoplasm (Figs. 36 and 79). These "shredded" MG were seen in both the laser-damaged areas (Figs. 30, 31, 53, 60, 61, 73, 79) and in the controls (Figs. 17, 36, 37, 47, 55, 64). They may be far more frequent in the laser-damaged cells and an investigation is under way to count them and compare the lesion cells to the controls, and to cells from peripheral RPE. Laser irradiation may increase their frequency.

Within the MB and the EL, the apical RPE border often (but by no means always) contains a very large number of large, newly-formed phagosomes with recognisable outer segment discs (Fig. 4); or packets of outer segment; discs are closely pressed to the apical surface, or partially inserted into the cell (Fig. 67) in some cases forming a distinct border zone (Fig. 60). Large phagosomes are also seen deeper in the RPE cell (Fig. 61). It seems that very soon after the laser irradiations there is a burst of outer segment disc shedding at a much enhanced rate.

Some mitochondria of the RPE may be swollen, with cristae reduced or absent. This is seen more often in the lesions (Fig. 23) and less often in the controls (Fig. 37). Some mitochondria may become very elongated, in the lesion (Fig. 80) and in the controls (Fig. 36). Some become crescent-shaped, surrounding large vacuoles or cystic spaces (Fig. 32), and are seen also in control areas (10 - 20 cells from the edge of the experimental lesions). It may be that intense light has an effect over a wider area than is delimited by the gross pathology of the lesion. In this connection we are currently examining peripheral areas of these retinas remote from the lesions. Often normal mitochondria are seen within laser damaged RPE cells (Figs. 29, 40, 57, 60, 61, 73).

The cells which show scalloping show fewer degenerative changes than do the humped cells, and the coagulated-exploded and reduced cells of the lesion centre show most damage effects. There is however a distinct end to the lesion, even though there is a gradation of damage within it from periphery to centre, where the palest cells are found.

Where the central cells are co-agulated and necrotic, and separated off from Bruch's membrane, the neighbouring less-damaged cells send basal extensions into the gap left by the loosened RPE cell, and these tongue-like

extensions appear to be closing this gap (Figs. 18, 53, 56, 59, 66). No mitoses were observed in this study.

The normal RPE cell contains an abundance of smooth endoplasmic reticulum (SER). In the light-damaged RPE, Kuwabara (1979) found that often the cisternae swell and the membranes of the SER then become closely appressed and form profiles of what looks like "pinched" SER. We see these profiles in some laser-damaged cells (Fig. 23) and also in some control areas (Fig. 25), but never in the severely damaged cells where very little cytoplasmic substructure is left (Fig. 53). It may be that our control areas are near enough to the laser irradiated zone to be affected by the light in the retina. A careful examination of the peripheral retina is being undertaken to see if "pinched" SER profiles can be seen there. In some RPE cells in some of the lesions, where the damage was not very destructive, the SER shows vacuolar dilatation of the cisternae.

The heavily damaged RPE cells contain large myelin-figures (Figs. 40 and 48), many dense inclusions, cystic spaces (Figs. 32 and 53).

There are also large cystic spaces between Bruch's membrane and the separating off or separated-off RPE cell (Figs. 28, 53, 68). While the damage effects are most marked in the marker burns, both in the number of cells involved and in the extent of the damage within the central lesion cells, one or two cells in the small experimental lesions often shows very similar damage patterns. Rarely, a cystic space is seen in a normal cell (Figs. 74 and 80).

Large autophagic vacuoles with many and diverse inclusions are seen most often in the RPE cells in the marker burns, and less frequently in the RPE cells of the experimental lesions (Figs. 30 and 31). These autophagic vacuoles sometimes contain melanin granules also.

We diligently searched all sections (by TEM) for striated rootlets. Schushereeba et al (1981) reported that there were 2.5 times the number of striated rootlets and centrioles in the RPE cell apex of retinas exposed to low level whole eye diffuse argon-irradiation compared to occluded eyes. We found very few striated rootlets in the RPE cells in all the material of this study.

In some of the EL, one MB and in two control samples there is seen what appears to be a condensation of amorphous material around the bases of the microvilli and in their crypts at the RPE apical surface (Figs. 17 and 64). Kuwabara (1979) refers to a similar dense granular material seen in a monkey exposed to strobe light for an hour and suggests that it might be proteinaceous or mucopolysaccharide material secreted by the RPE. Since this is seen in MB, EL, and control areas it does not appear to be related to the effects of lased irradiation.

In summary, the RPE cells within the laser affected areas showed an absence or reduction of their basal infolds, and they contained an increased number of inclusion bodies, probably lysosomes and lipofuscin granules. Cells of the lesion centre often appear paler than the normal RPE cells or the cells of the lesion periphery. These latter often seem to be rather dark-staining. MG are reduced in number, and the orientation is altered.

#### The outer segments

The distal portions of the OS show various signs of disturbance. In normal tissue the central zone only of the outer segments may often show convolutions and foldings, but the discs within these convolutions are normal (Marshall et al, 1979). This "twisting and folding" is reported also

by Lund et al (1981) in both laser affected and control material.

In some samples the outer segments are very straight, even within the experimental lesions (Figs. 19, 50, 57) whereas in other cases, the outer segments have a unit of whorled discs at their proximal ends both in the controls (Figs. 24, 42, 45) and the lased areas (Figs. 33, 41). There is a good deal of variation within one macula of one eye in the appearance of the OS. Not all are equally affected. Some OS are very swollen and have lost almost all their discs; others show damage restricted to the proximal OS. In some experimental lesions, only the distal OS ends were affected. In the marker burns, however, the outer segments tended to be irregularly swollen and the disc stacks tended to be disorganised and pyknotic, but as in all lesions, the degree of damage often varies between neighbouring outer segments.

Apart from the disc packets which attach to and insert into the RPE cell, the OS distal tips are distant from the damaged RPE apical border. In the experimental lesions this is often very clearly displayed. The OS tips lie very close to the apical ends of the normal RPE cell neighbouring the laser-damaged RPE cells (Figs. 19, 20, 66, 71) while they are distant from many of the most damaged RPE cells in the EL centres (Figs. 19, 20, 66, 71, 77) but not from all (Figs. 27, 50, 52, 58).

In the control areas, the distal OS ends are almost always closely appressed to the apical borders of the RPE cells (Figs. 17, 34, 43, 46, 55, 64) but not always so (Fig. 74).

In both the control areas (Figs. 24, 42, 45, 75) and in the experimental lesions (Figs. 22, 33, 41, 52) there are a few areas where the outer segments have one whorled group of OS discs at the proximal end,

in the neighbouring zone the discs are disorganised (Figs. 22 and 24), but the rest of the outer segments contain normal disc stacks (Figs. 42, 45, 52). This might be ascribed to local differences in fixation effects; or to an idiopathic phenomenon; or to the effects of the laser on both the lesion, and its immediately neighbouring area. Very occasionally, re-arranged and distorted discs were seen in one OS in the control area (Fig. 16). In the MB the outer segments were much more often disorganised (Figs. 1, 7, 10, 11).

The most distal portions of the outer segments usually show a normal stack of outer segment discs (Figs. 46, 50, 51, 53, 54, 57, 58, 64, 65, 71, 77) in both the EL and in the controls, but there are exceptions (Fig. 63).

#### The inner segments (IS)

In the MB, some IS and their mitochondria seem to be very swollen (Figs. 3, 5, 7, 10, 11, 13, 14) or pyknotic (Figs. 3, 5, 7, 10, 11, 12) and they showed signs of general necrosis (Figs. 10, 11, 12, 14). Electron dense bodies of varied shapes are seen within the mitochondria of the IS in the EL, the MB and the controls (Figs. 3, 22, 24). They may be fixation-induced.

The striated rootlet of the IS is frequently seen in all the samples. It is obviously a very resistant organelle, as it shows no apparent alterations even when the mitochondria are swollen, contorted or pyknotic, or the background cytoplasm unusually electron dense (Fig. 3). It is found with the same frequency in the EL and the controls (see Table I).

In general, the myoids are less damaged than the ellipsoids but a few myoids in the MB contain large cystic spaces (Fig. 12).

I have often seen in previous studies small collections of tubular structures, forming "tubule-complexes" in the PR synaptic terminals, especially in the pedicles. In this study, these have also been seen not only in the PR synaptic terminals in both the controls and the experimental tissues, but also in the IS ellipsoid, among the mitochondria; in the IS myoid, immediately vitreal to the OLM; and once in one of the Henle fibres. I mean to examine these at high magnifications and measure them. It seems that they could be regions of SER that have undergone changes, or microtubular alterations.

In general, the state of the IS mitochondria in the EL varies a great deal, even in neighbouring photoreceptors of one lesion. Apart from swelling of mitochondria and loss of cristae, the IS in the EL are very little affected by the irradiation and appear relatively normal. In the MB the IS and their mitochondria are variously swollen, or pyknotic and generally disrupted (Figs. 2, 3, 5, 7, 9, 10, 11, 12, 13, 14).

Striated rootlets

Striated rootlets were so rarely seen in the RPE that it was not sensible to try to count them.

Striated rootlets seen in the inner segments in both laser-exposed areas and in their control areas were counted. The control areas were about 500  $\mu\text{m}$  distant from the lesions. About 30 photoreceptors were scored in each lesion area. Any portion of a striated rootlets seen, viewed in the TEM at a magnification of 4,000 x, was scored as positive.

TABLE I

Percentage of IS showing striated rootlets

	In lesion areas	in control areas
Foveal region	43	47
extra foveal region of the macula	46	44

Note that the proportion of striated rootlets seen in the fovea, with its concentration of cones, is similar to that seen extrafoveally where there is a preponderance of rods.

Small striated rootlets are also seen, commonly, in the Müller cells, in the area immediately vitreal to the OLM.

### The Müller cells

In the MB there is considerable swelling and edema in the ONL, involving the Müller cells all the way to the OLM (Figs. 2, 6, 9, 15). This is not apparent in the EL. In both the MB and the EL the Müller cells in the ONL contain many myelin figures, dense bodies and autophagic vacuoles. Could Müller cell edema account for the clouding seen by Beatrice et al 1977?

### The Synaptic terminals (ST)

The ST do not appear to be morphologically affected by the laser irradiations of this study.

### The Henle fibres

In two foveal lesions a few elongated pyknotic inclusions are seen in the Henle fibres, or in the MB in the Müller cells alongside the Henle fibres (Fig. 8).

TABLE II  
SIZES OF THE LESIONS

Neodymium pumped dye laser, operating at 10Hz, pulse duration ~ 10 n sec;  
enucleation 1½ hours post-irradiation (Eye 2T, animal 266M 12:30 pm) λ 900 nm.  
(Eye 2U, animal 8703 2:30 pm) λ 867 nm.

2U: D				2U: S			
lesion number	(~ ED <sub>50</sub> ) Dose, μJ	max. diameter of lesion (D) μ	Estimated number of RPE cells in D.	lesion number	Dose, J (~ 3xED <sub>50</sub> )	max. diameter of lesion (D) μ	Estimated number of RPE cells in D
1 .				1	15.2		
2				2 .	15.7	88 x	7
3				3 .	16.0	54 x	3-4
4 .				4 .	15.6	121	11
⑤ .	5.9	115	9	⑤ .	13.6	74	6-7
6 .				6 .	17.3	84	9-10
7				7 .	15.7		
8 .				8 .	16.9		
9				9	14.8		

2T: D				2T: S -no markers			
1	6.2			1 .	17		
2 .	6.2			2	17.2		
3 .	7.3			3	13.2		
4	6.6			4 .	17.2		
⑤ .	6.2	100	9	⑤ .	16.6	70	6
6	7.5	96	8	6 .	19.3		
7 .	7.6	80	6-7	7	13.5		
8	7.3			8 .	13.5		
9	7.8			9	14.4		

Lesions ⑤ are foveal.

. = these lesions were visible ophthalmoscopically at 1 hr.

In all the eyes, except 2TS, the lesions were surrounded by 12 marker burns.

x = There were problems in isolating some of the lesions under the dissecting microscope, and as a result lesion 3 might be lesion 9, and lesion 2 and 8 might be interchangeable.

TABLE III

## COMPARISON OF FOVEAL LESIONS

lesion specification	dose $\mu\text{J}$	wavelength nm	largest diameter of lesion $\mu$	number of RPE cells along the largest diameter	position of the lesion in fovea	number of pyknotic PR nuclei in lesion	COMMENTS
TD lesion 5	6.2	900	100	9	at edge of clivus, in the pit	1	appears to show most changes in the RPE and a few necrotic IS
UD lesion 5	5.9	867	115	9	on pit floor, just off centre	2, markedly pyknotic	
TS lesion 5	16.6	900	70	6	on pit floor	1	
US lesion 5	13.6	867	74	7	at edge of clivus, in pit	none	This lesion appears to display least damage of the 4 lesions

TD } Animal 266M  
 TS }

UD } Animal 8703  
 US }

Compared to the controls, the lesions show considerable disturbances in cells of the RPE, some changes in the OS, and one or 2 pyknotic PR nuclei. All the controls show a clear zone of well developed RPE basal infoldings. In all the lesions these are absent or reduced in extent and number. Whorls of discs are present in the lesions and in the controls at the proximal ends of the OS. No pyknotic PR nuclei were seen in control tissue.

There is a similarity between the lesions that result from similar doses ( $\mu\text{J}$ ). (TD and UD =  $\sim\text{ED}_{50}$ ; TS and US =  $\pm 3 \times \text{ED}_{50}$ ). The small difference in the wavelength may not be significant but lesions are slightly larger at the  $867\mu$  wavelength.

The effects of laser irradiation are restricted to the outer retina, with the RPE the most severely affected. The lesions are all similar, and quite small. The small differences observed may well lie within the variations expected because of very local variations within the tissue. The left eyes which hold the threshold lesions seem to show slightly greater damage than the right eyes, with the superthreshold lesions.

## COMMENTS ON THE RESULTS

Adams et al (1974) described the lesions produced by a gallium arsenide laser as toroids when seen ophthalmoscopically, consisting of a well-defined opacity surrounding small central circles of lesser opacity. Their laser produced a pulse train of 500 nanosecond pulses at a 120 KHz repetition rate and emitted 20 - 130 milliwatts of power at 8,600Å. The laser used in our study operated at 10 Hz, single pulses of 10 n second duration with pulse energies of ~5 µJ - 19 µJ for the EL and 100 pulses at 15 µJ or 50 µJ for the MB at 8670Å. They looked at the lesions by flat mounts and by LM, 1 hour post irradiation. The lesions in our study were much smaller and we did not see the dough-nut effect (toroid) in the pigment epithelium of central unaltered RPE surrounded by a concentric zone of destruction. They saw central sparing in the lesions. What we did see was a different sort of toroid, of pale, depigmented, swollen vacuolated PE cells centrally, surrounded by a concentric zone of dark-staining RPE cells less severely affected than the central cells of the lesion.

However, in both studies the damage is centered mainly in the pigment epithelium, and to a lesser extent, in some outer segments, with the inner retinal layers unaffected. They saw major changes in Bruch's membrane and the choroid, while we saw only small changes.

In the study by Adams et al (1974) the lesions were at ED<sub>50</sub> and 2 x ED<sub>50</sub> levels of power. They found the latter produced a lesion of 280 µ, as compared to 160 µ in the former, and created more destruction. Their smallest lesions (ED<sub>50</sub>) were found to be difficult to detect and very small (25µ), and showed only by swelling, necrosis and destruction of a few PE cells and vacuoles in the subretinal space. Their lesions showed greater pathology after 24 hours. No humping or peaking of the outer retina

was observed in either their study or ours, such as is seen in many studies when argon, krypton or ruby lasers are used. They found the lesions to be circular even though the gallium arsenide laser emits a beam in the shape of an elongated ellipse.

Beatrice et al (1977) used a gallium arsenide laser operating at 1600 Hz or 132 Hz with exposure durations of 1.0 sec - 90 secs, and a peak pulse power of 1 watt to 10 watts. At the exposure sites they saw ophthalmoscopically, a pale grey clouding within 10 seconds of initiation of the exposure which persisted for 24 hrs but they could find no histologic or fluorescein leakage correlate. If comparable at all to this study, then the appearance of the pale PE cells in the lesion centre together with the vacuolar spaces between the PE and Bruch's and the edema in the MC are possible correlates of the clouding seen by Beatrice et al (1977), but not confirmed in other studies (Lund et al 1981)

Tso (1979) makes reference to the ability of the RPE to proliferate or slide in to cover RPE portions left bare after laser or photocoagulation radiation has created mild lesions. In the centre of the lesions in our study some RPE cells are detached from Bruch's membrane, and the space left behind is bowl-shaped because the RPE cells that lie alongside the denuded area of Bruch's membrane send the thin basal extensions which reline Bruch's membrane.

Melanin granules described by Kuwabara (1979) as "shredded", when damaged by light, are seen in the RPE in this study in the experimental lesions and in the control tissues. The peripheral retina is being examined for these because it is possible that the control areas are near enough to the laser damaged areas to suffer some changes from the light in the retina.

## SUMMARY

Both MB examined in detail were from the same eye (2TD), MB 11 from the peripheral retina at the temporal edge of the macula and MB 9 from the peripheral retina at the inferior edge of the macula. MB 11 is more severe than MB 9 in the extent of the damage, and shows blood in the subretinal space.

The damage level is greater in all respects in the marker burns than in the EL. More cells are involved in each zone, the RPE cells tend to be more affected and the lesion extends from the vitreal end of the choroid to the OPL. Red blood cells seen in the subretinal space and over the disrupted RPE cells of the lesion centre gain access through a breach in Bruch's membrane in MB 11. In all the lesions, the most centrally located RPE cells are most affected and appear paler than the other RPE cells in the lesion.

In the EL the damage seen is essentially restricted to the cells of the RPE. No two lesions are identical in appearance, but they are similar. The basal infolds are always affected, so are the microvilli, which become variously retracted, or fragmented, or swollen and fused. MG are usually absent from the MV or cell apex in the lesion centre, but not always. The cytoplasm becomes vacuolated. The central lesion cells are usually reduced in height, and pale.

FIGURE LEGENDSFigs. 1 - 8 MB 11, Eye 2TD

- Fig. 1 TEM x 2,000 The RPE is coagulated and the nucleus necrotic. Blood is seen in the subretinal space. OS are irregular, displaced and the discs disorganised.
- Fig. 2 LM x 1,200 The lesions extends from the RPE through to the OPL. The area of the ONL containing the pyknotic PR nuclei is very edematous and it bulges into the OPL. Blood lies in the subretinal space among disorganised OS.
- Fig. 3 TEM x 8,000 A cone IS displays swollen mitochondria with disorganised cristae and pyknotic inclusions. Rod IS are pyknotic and irregular in outline, but their striated rootlets appear intact.
- Fig. 4 TEM x 6,700 A scalloped RPE cell apex contains many large phagosomes with OS discs. Microvilli are reduced to only a few fragments. One OS in the subretinal space is disorganised and surrounded by whorled microvillous processes.
- Fig. 5 TEM x 10,000 Necrotic rod inner segments seen in the ONL.
- Fig. 6 TEM x 2,700 ONL showing border area between deeply pyknotic and shrunken PR nuclei, lightly pyknotic PR nuclei and normal ones. There is swelling in the intercellular spaces as well as in Müller cells. Perinuclear cytoplasm is vacuolated.
- Fig. 7 TEM x 4,000 Rod and cone IS and OS. Note the very swollen cone IS containing mitochondria with cristae; a few very necrotic rod IS with few recognisable organelles and relatively normal OS; the disorganised OS, especially one rod OS; and a whorled mass of OS discs in the proximal part of the OS.
- Fig. 8 TEM x 4,000 ONL showing pyknotic PR nucleus and pyknotic bodies in the Müller cells between the PR fibres.

Figs. 9 - 15 MB 9 - EYE 2TD

- Fig. 9 LM x 1,200 The lesion is seen extending from the RPE [which is very reduced in height in the lesion centre and has a scalloped apical border in the lesion periphery] to the OPL.
- Fig. 10 TEM x 1,400 Detail of portion of the lesion showing the pathology in the IS, OS, and RPE.
- Fig. 11 TEM x 2,700 Swelling pyknosis and necrosis in the IS. Two IS contain whorled or wavy membrane complexes.

- Fig. 12 TEM x 2,000 Cone myoids are generally less affected than the ellipsoids, but there is a very large cystic space near the OLM. Rods show a greater degree of pyknosis than do the cones.
- Fig. 13 TEM x 10,000 Portion of a cone ellipsoid showing a variety of changes in the mitochondria.
- Fig. 14 TEM x 5,000 Neighbouring PR inner segments show different degrees of swelling and different forms of mitochondrial changes. One has very swollen mitochondria with cristae almost entirely absent and another has shrunken and pyknotic mitochondria.
- Fig. 15 TEM x 2,700 Pyknotic PR nuclei surrounded by disintegrating cytoplasm which appears to be pale and granular or very electron-dense.

Figs. 16, 17 Control areas for MB 9

- Fig. 16 TEM x 2,700 One outer segment shows disc disorganisation and a few OS are convoluted in their mid-zones (a common finding), with intact discs. Inner segments are normal. Microvilli are abundant and contain melanin granules.
- Fig. 17 TEM x 10,000 RPE has an even apical border, with well developed microvilli containing elliptical or oval melanin granules (MG). Condensations of a dense material can be seen around some of the microvilli and in their crypts. An OS tip lies close to the RPE apical border. A large "shredded" MG can be seen in the RPE cell.

Figs. 18 - 23 Foveal lesion, Eye 2TD (~ED<sub>50</sub>, 900 nm)

- Fig. 18 LM x 1,300 The lesion centre contains RPE cells extruded from Bruch's membrane leaving a bowl shaped space. Neighbouring RPE cells extend tongues of tissue to cover the gap left by the extruded cells, which look paler than the attached cells. The other RPE cells of the lesion show marked scalloping of the apical border.
- Fig. 19 TEM x 1,400 Details of the RPE cells displaying humped and scalloped apical borders. Note a clump of swollen and fused microvilli between two "humped" cells. The microvilli tend to lack MG. OS appear normal.
- Fig. 20 TEM x 2,700 Another section through the lesion showing the disorganised pale RPE cell at the lesion centre; much reduced in height and bearing swollen and fused microvilli. The neighbouring cells stain darkly.

- Fig. 21 LM x 1,300 Compare this to Fig. 18 - another section giving a slightly different view of the lesion centre.
- Fig. 22 TEM x 2,700 Most of the cone inner segments (IS) are not much affected (the mitochondria are a little swollen) but one IS shows necrotic changes. The proximal outer segments (OS) contain a unit of whorled discs and the neighbouring discs are not normal (compare with Fig. 24, control section).
- Fig. 23 TEM x 6,700 Details of two RPE cells in the lesion centre; one is very electron dense, the other relatively pale. Note the form of the smooth endoplasmic reticulum (SER), the absence of basal infolds, vacuolar spaces, "halos" around the MG and the mottled appearance of Bruch's membrane.

Figs. 24 and 25 - Control areas for lesion shown in Figs. 18 - 23.

- Fig. 24 TEM x 2,700 Compared to Fig. 23. The two are very similar, except for the presence of one necrotic IS in Fig. 23.
- Fig. 24 TEM x 6,700 Normal RPE showing profiles of "pinched" SER. Compare with Fig. 23

Figs. 26 - 33 Foveal lesion Eye 2UD (~ED<sub>50</sub>, 867 nm)

- Fig. 26 LM x 1,200 The lesion is seen in the fovea at the margin of the foveal pit and clivus. It appears to affect only the RPE.
- Fig. 27 TEM x 1,400 RPE at lesion centre shows a pale, vacuolated cell with retracted MV and no basal infolds. Small vacuolar spaces are seen at the base of the cell. MG are present in the neighbouring lesion cell.
- Fig 28 TEM x 14,000 and Fig. 29 x 10,000 The basal part of an RPE cell in the lesion centre showing coagulated cytoplasm, cystic spaces, no basal infolds. There are a few mitochondria with cristae. Bruch's membrane has a dense and mottled appearance. A large membrane bound cyst is seen at the cell base. The endothelial cell has processes extending into Bruch's membrane.
- Fig. 30 TEM x 10,000 and Fig. 31 x 20,000 Details of one RPE cell, lesion centre, showing a large membrane-bound body, probably an autophagic vacuole, a "shredded" MG, a pyknotic nucleus, and many melano-lipofuscin granules. A large phagosome is present.
- Fig. 32 TEM x 14,000 Portion of a RPE cell in the lesion periphery showing a few basal infolds and a very large cystic space enclosed by what is probably an elongated mitochondrion.
- Fig. 33 TEM x 4,000 IS and OS of the lesion area. Compare with Figs. 22 and 23 of the fovea of eye 2TD. They are very similar.

Figs. 34 - 37 Control areas for lesion shown in Figs. 26 - 33

- Fig. 34 TEM x 2,000 Normal RPE. Compare with Figs. 27 - 31 of the lesion RPE.
- Fig. 35 TEM x 6,700 Cone IS show some mitochondrial swelling (perhaps somewhat less than in the lesion) and they also contain pyknotic mitochondrial inclusions (see Figs. 22, 23 and 33).
- Fig. 36 TEM x 20,000 and Fig. 37 x 10,000 Portion of RPE cell displaying normal nucleus; basal infolds; melano-lipofuscin bodies; some swollen mitochondria; some normal mitochondria and some elongated mitochondria; "shredded" MG (one surrounded by a rim of dense cytoplasm suggesting it may be an autophagic vacuole).

Figs. 38 - 43 Foveal lesion Eye 2TS (~3 x ED<sub>50</sub>, 900 nm; no surrounding MB).

- Fig. 38 LM x 1,200 A general view of the lesion showing a portion of an extruded RPE cell and the scalloped apical border. The effects of the lesion are confined to the RPE, Bruch's membrane and the OS.
- Fig. 39 TEM x 2,700 A RPE cell shows reduced height, a tongue of extruded tissue composed of swollen and fused microvilli which encloses cell debris. MG are absent from the MV.
- Fig. 40 TEM x 10,000 Basal part of the RPE cell contains many myelin figures and pyknotic bodies. There are no basal infolds.
- Fig. 41 TEM x 5,000 The OS in their mid-zones are irregular in shape and contain discs in whorls, fragmented discs, re-arrangements of discs in disarray, and discs which are vesiculated.

Figs. 42, 43 Control tissue for foveal lesion 2TS

- Fig. 42 TEM x 4,000 The IS have the same appearance as those seen in Fig. 41. Only the most proximal parts of the OS contain whorled and other forms of disturbed discs. The extent of these alterations appears to be less than in the lesion (see Fig. 41).
- Fig. 43 TEM x 2,000 Normal RPE from fovea - note some folding of OS.

Figs. 44 (LM), 48 - 51 (TEM) Foveal lesion from eye 2US (~3 x ED<sub>50</sub>, 867nm)Figs. 45 - 47 Control tissue for foveal lesion 2US.

- Fig. 44 LM x 1,200 The lesion is in the foveal pit and appears to affect the RPE only. Note that the RPE cells in the lesion centre look paler than their neighbours.

- Fig. 45 TEM x 5,000 In the control areas (10 - 20 cells distant from the lesion centre) there are whorls of outer segment discs in the proximal parts of the OS and one OS is irregular in outline and has disintegrated proximal discs.
- Fig. 46 TEM x 5,000 The RPE is normal. Note MV with elongated MG, basal infolds, the cone outer segment at the apical border, and the large number of densely-staining inclusions.
- Fig. 47 TEM x 10,000 The RPE cell contains several "shredded" MG in various forms.
- Fig. 48 TEM x 20,000 Part of RPE cell in lesion centre containing many cystic spaces with pyknotic outlines, a phagosome, and sparse basal infolds.
- Fig. 49 TEM x 5,000 Basal part of RPE cell and mottled Bruch's membrane. Some of the sparse basal infolds contain amorphous material. The cytoplasm is vacuolated.
- Figs. 50 and 51 TEM x 1,400 Two views of cells in the lesion centre. The lesion contains some pale staining cells and some electron dense cells. Outer segments reach to the apical border. MG are absent from the apical RPE border in the lesion centre where the MV are retracted or swollen and fused. Some scalloping of the apical RPE border is seen.

Figures 52 and 53, Macular lesion 6, Eye 2TD

- Fig. 52 TEM x 1,400 A general view of the area of the lesion. The outer segment discs are in normal array in their distal parts.
- Fig. 53 TEM x 5,000 The central RPE cells of the lesion show reduction in height, coagulated cytoplasm, pyknotic nuclei, and cystic spaces basally. Basal infolds are absent. Normal looking OS insert into the apical cell border, from which microvilli are absent. The neighbouring cells, within the lesion, extend tongues of tissue basally along Bruch's membrane under the disorganised disburbed cells of the lesion centre.

Figures 54 and 55, TEM controls for macular lesion 6, Eye 2TD

- Fig. 54 TEM x 2,700 Normal RPE.
- Fig. 55 TEM x 10,000 A "shredded" MG in the normal RPE cell.

Figures 56, 59, LM, Figures 57, 58, 60 - 63 TEM Macular lesion 7 from Eye 2TD

- Fig. 56 and Fig. 59 LM Two different thick sections through the lesion centre. Fig. 56 shows MG in the MV of the extruded RPE cell, an unusual finding. Note the tongues of tissue from RPE cells that

move towards each other to close the gap left by the extruded RPE cells in the centre of the lesion. The scalloping of the apical border in the lesion is relatively gentle.

- Fig. 57 TEM x 6,700 RPE cell in the lesion periphery, showing a gently scalloped apical margin and 2 large "shredded" MG, which appear to be necrotic. An extruded mass of MV can be seen between the OS. The basal infolds are very reduced.
- Fig. 58 TEM x 1,700; Fig. 60 TEM x 5,000; and Fig. 62 TEM x 8,000 .  
 Fig. 60 RPE cells in the lesion show membranous material in the disturbed  
 Fig. 62 cell, probably derived from retracted MV. Note the absence of basal infolds. Fig. 60 shows a large number of OS disc packets on the apical RPE cell surface, and within the apical cytoplasm. Note the pyknotic nucleus.
- Fig. 61 TEM x 6,700 A RPE cell from the lesion area has a "shredded" melanosome and an elongated MG in the basal part of the cell. Basal infolds are absent. A large phagosome of OS discs can be seen.
- Fig. 63 TEM x 5,000 RPE cell in lesion displays a mass of fused MV. Some of the OS tips near the RPE apical border are pyknotic and have discs in disarray. A shredded MG is present.

Figs. 64 and 65 Control areas for lesion 7, Eye 2TD

- Fig. 64 TEM x 8,000 There are 3 large and 1 small "shredded" melanosomes and a large number of melano-lipofuscin bodies in the RPE cell. Note the association between the OS tips and the microvilli and the apical border of the RPE cell. Dense condensations of amorphous material are seen around the microvilli.
- Fig. 65 TEM x 4,000 The OS are somewhat twisted, and disc regularity a little disturbed. One OS is markedly swollen and the discs fragmented and partly vesiculated.

Figs. 66 - 69 Lesion 4 of Eye 2US

- Fig. 66 TEM x 2,700 RPE cell in lesion centre contains oriented elongated MG within a complex network formed from swollen and fused microvilli. Between this complex and the rest of the cell beneath it there has developed a space. The central cell of the lesion is pale and is contained in a bowl-shaped space outlined by tongue-like extensions from the neighbouring cells of the lesion. MG are seen in the swollen fused microvillous mass.
- Fig. 67 TEM x 4,000 On the lateral border between the pale vacuolated cell of the lesion centre in the RPE and its neighbouring cell in the lesion there can be seen an area containing a group of ~parallel membranes, which extend to the basal area of the cell in a less organised way.

- Fig. 68 TEM x 14,000 Detailed view of the basal part of a RPE cell and Bruch's membrane in the lesion centre. In some swollen mitochondria some cristae can still be seen. The basal part of the RPE cell is very cystic. Bruch's membrane contains electron dense material.
- Fig. 69 TEM x 4,000 A portion of the choroid, under the lesion, is displayed. A melanocyte shows considerable necrosis and disorganisation. This was a unique finding.

Figs. 70 - 73 Lesion 6 in Eye 2US

- Fig. 70 LM x 1,300 The OS are "knobbed" in their mid-regions. The RPE is scalloped on its apical margin except in the centre of the lesion. The central cells are separated from Bruch's membrane.
- Fig. 71 TEM x 1,400 The OS distal ends are normal and reach to the PE except in the lesion centre where the RPE cell is shrunken, vacuolated and reduced in height. Melanin granules can be seen in the apical parts of the damaged RPE cells.
- Fig. 72 TEM x 4,000 Note the disorganised cytoplasmic matrix which contains many electron dense bodies. There are neither basal infolds nor MV present.
- Fig. 73 TEM x 6,700 The photomicrograph shows the amount of membranous material often seen in the central cells of the lesion in the RPE.

Figs. 74 and 75 Control tissue for lesion 6 Eye 2US

- Fig. 74 TEM x 2,700 Normal RPE.
- Fig. 75 TEM x 2,700 Normal IS and OS. Note the presence of whorled discs in the proximal OS.

Figs. 76 - 79 Lesion 3 or 9 of Eye 2US

- Fig. 76 TEM x 1,300 This shows an extruded RPE cell and the scalloping of the RPE apical border.
- Fig. 77 TEM x 2,700 The outer segments are distant from the expanded mass of fused microvilli that extends into the subretinal space.
- Fig. 78 TEM x 6,700 Another view of the microvillous mass which encloses MG and outer segment discs.

- Fig. 79 TEM x 20,000 Apical parts of RPE cells, at the lateral cell border. Note the SER, the melano- lipofuscin bodies and the large "shredded" melanosome enclosed by a bordering rim of dense material.
- Fig. 80 TEM x 2,700 Normal RPE from control tissue. Note the polarity of the cell with relation to the cell organelles. The MG are in the apical MV, melano-lipofuscin bodies occupy the central zone. The mitochondria and the basal infolds are basal. Some mitochondria are very elongated.



1



2



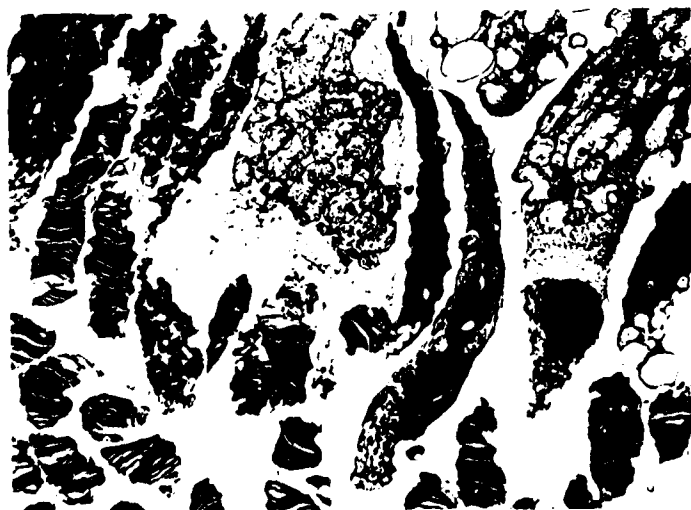
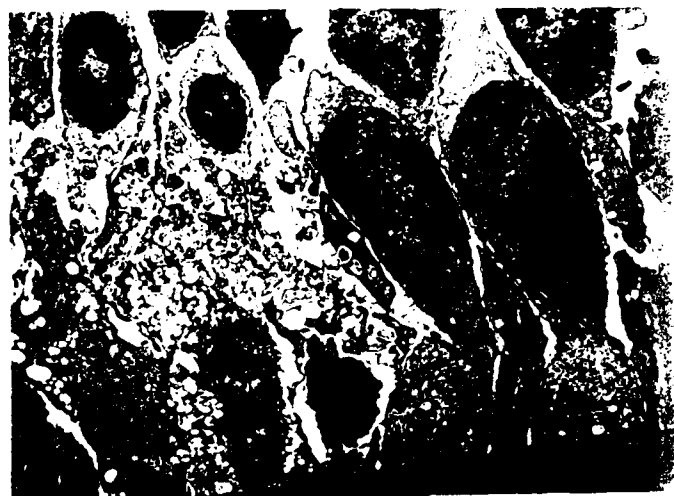
3



4



5



7





9



10



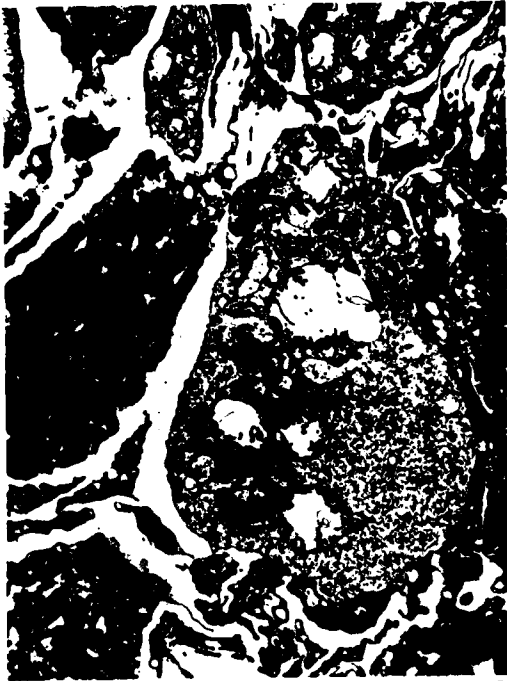
11



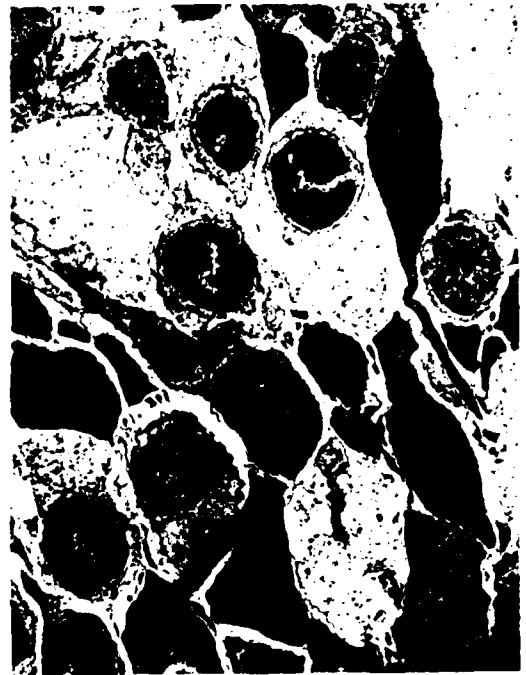
12



13



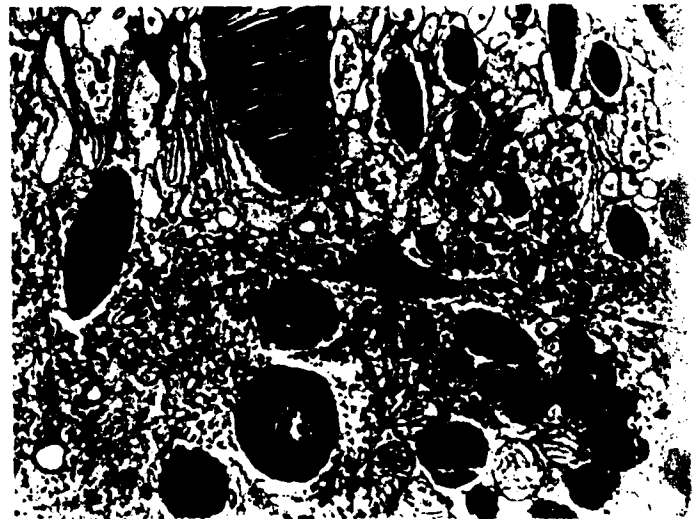
14

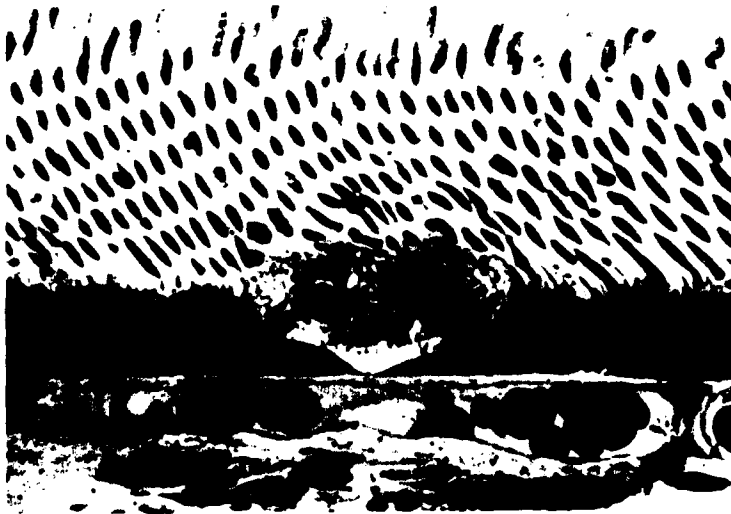


15



16c

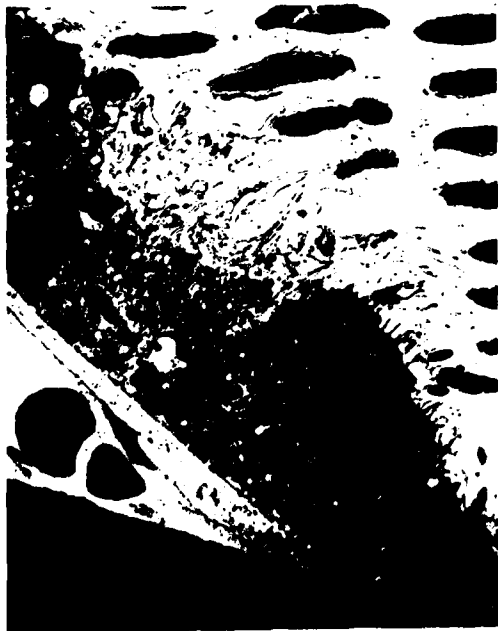




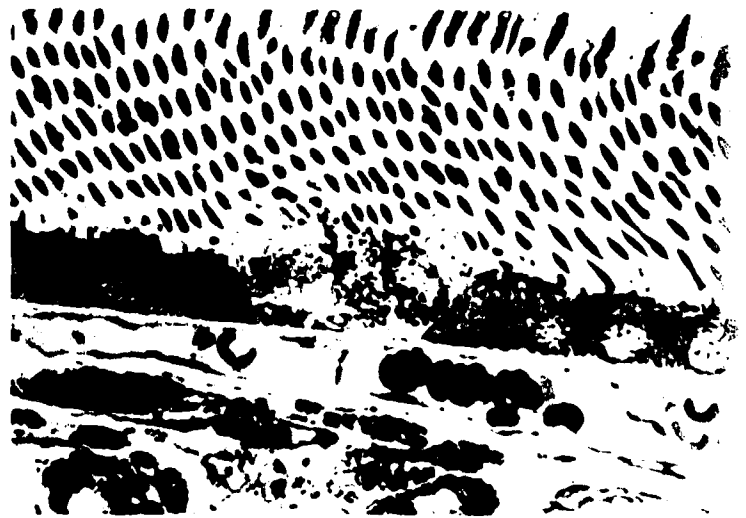
18



19



20



21



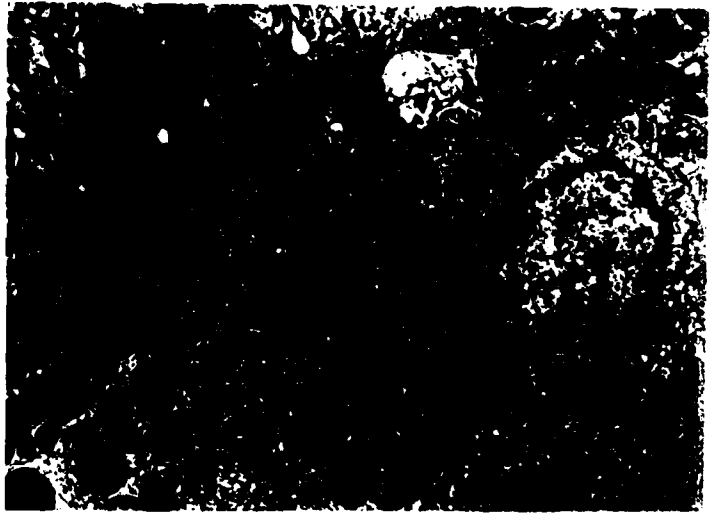
22



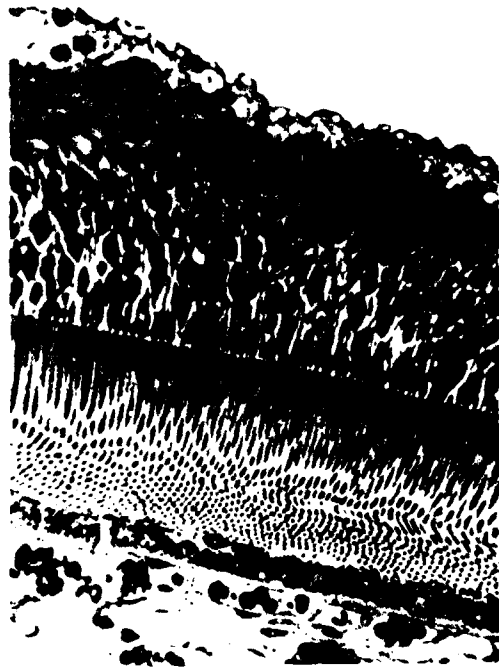
23



24c



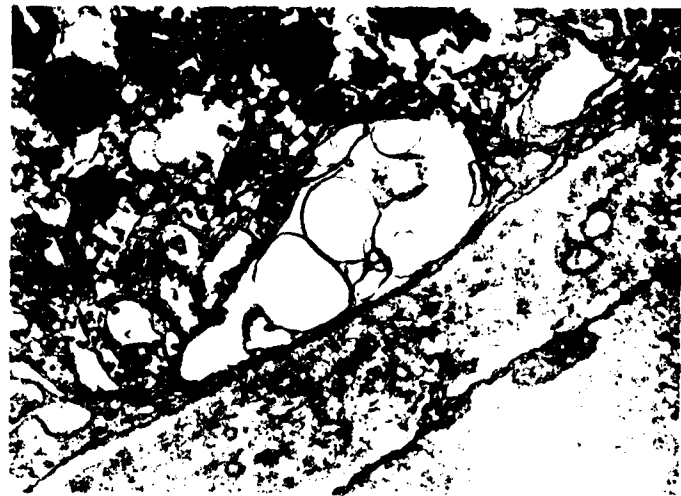
25c



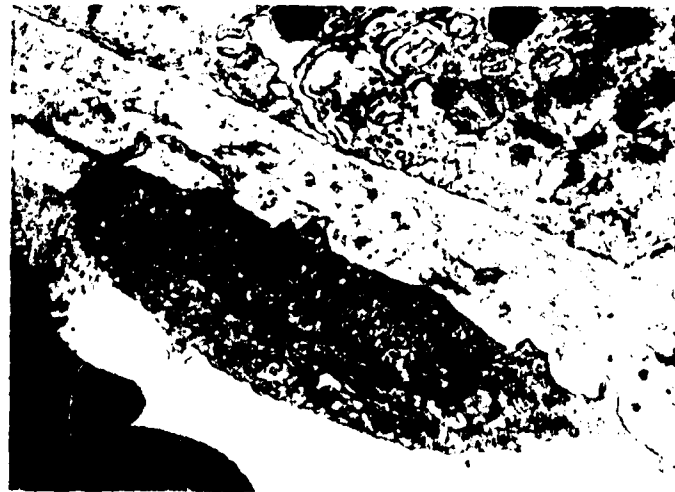
26



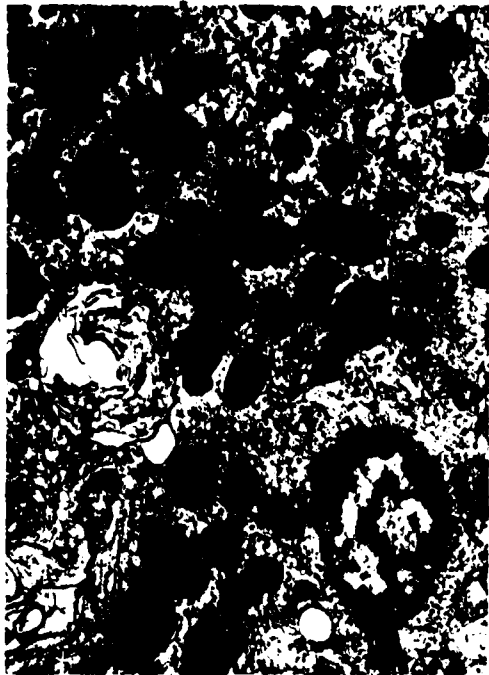
27



28



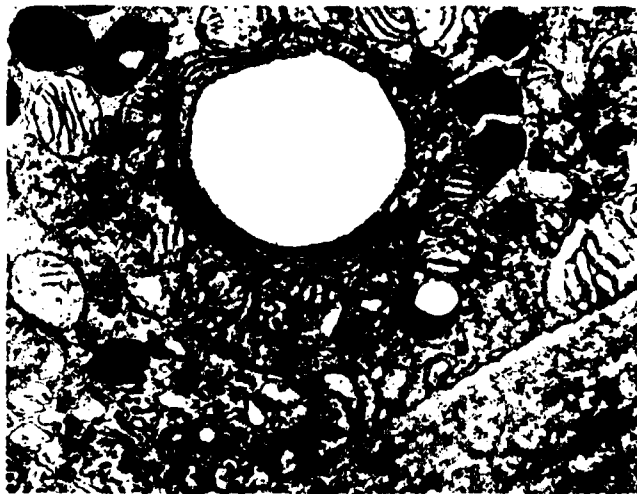
29



30



31



32



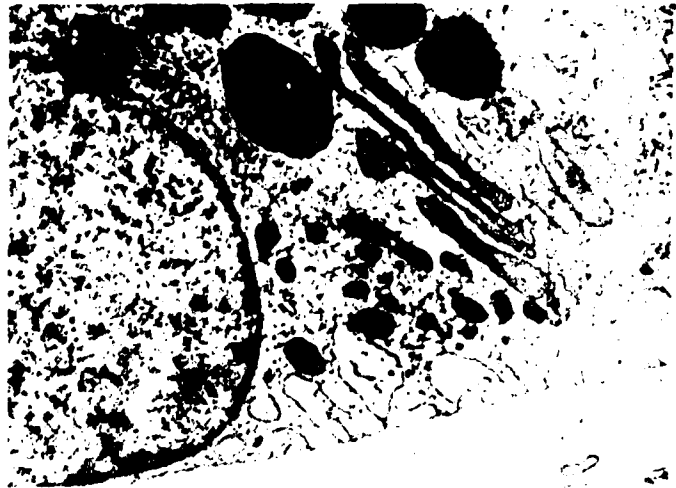
33



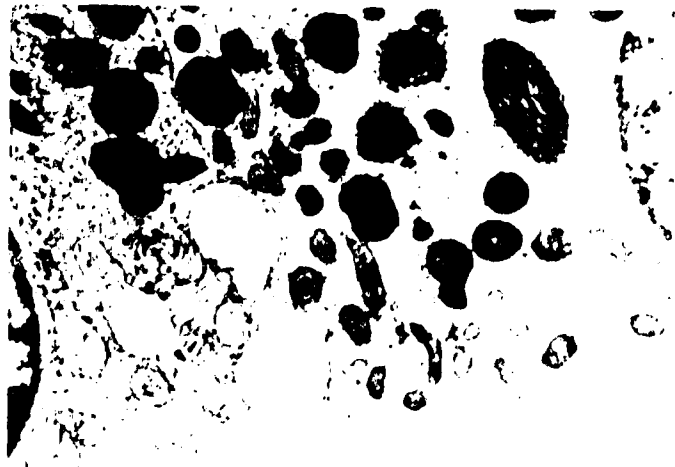
34c



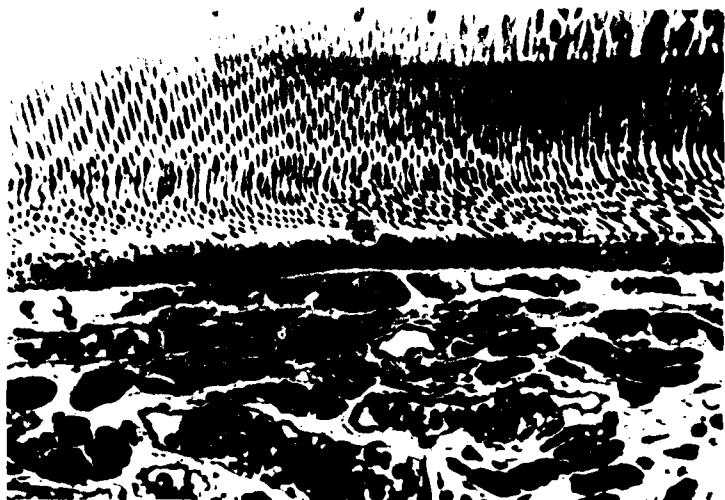
35c



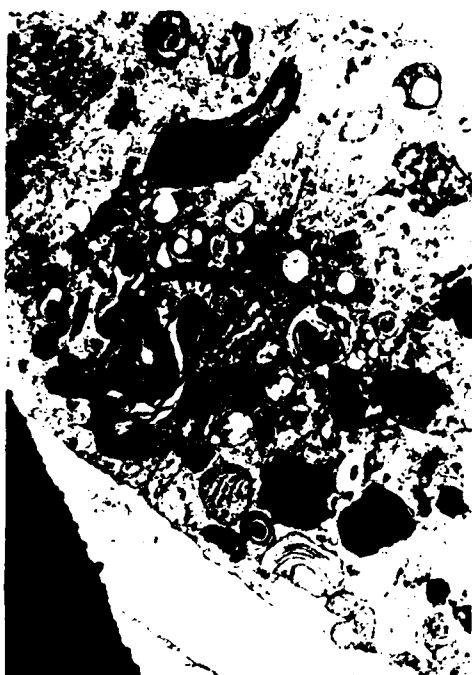
36c



37c



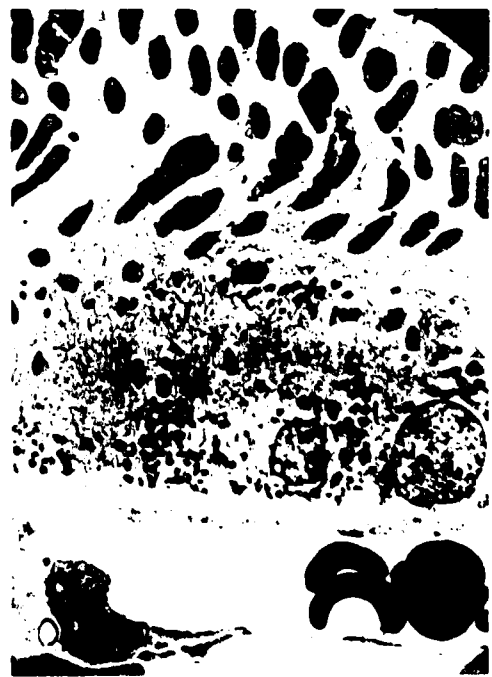
38

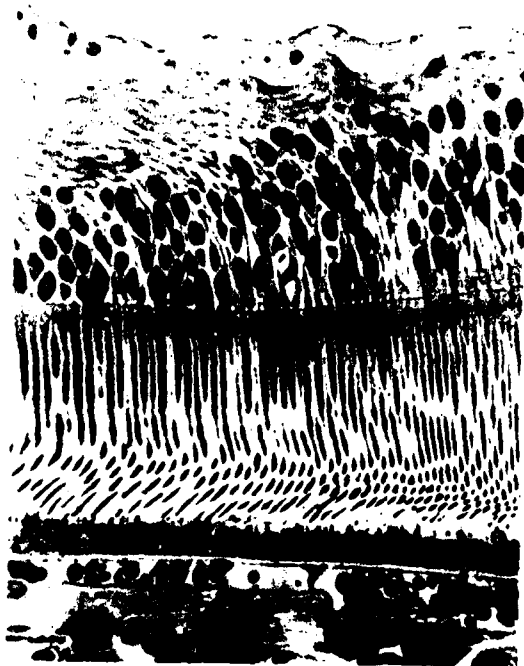


40



42c





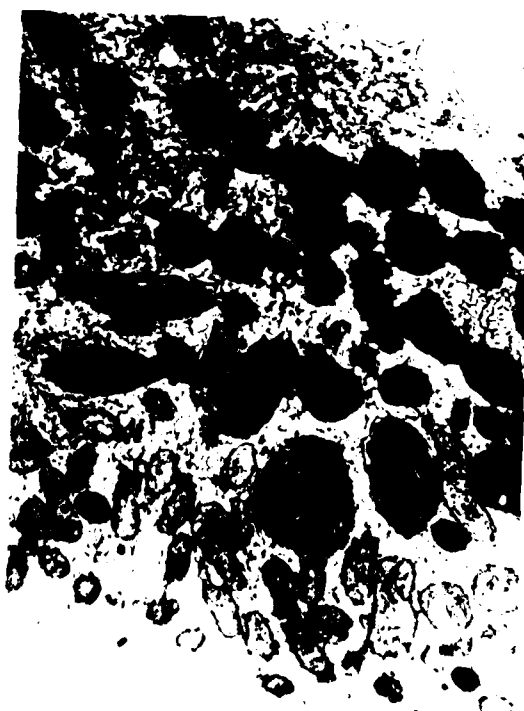
44



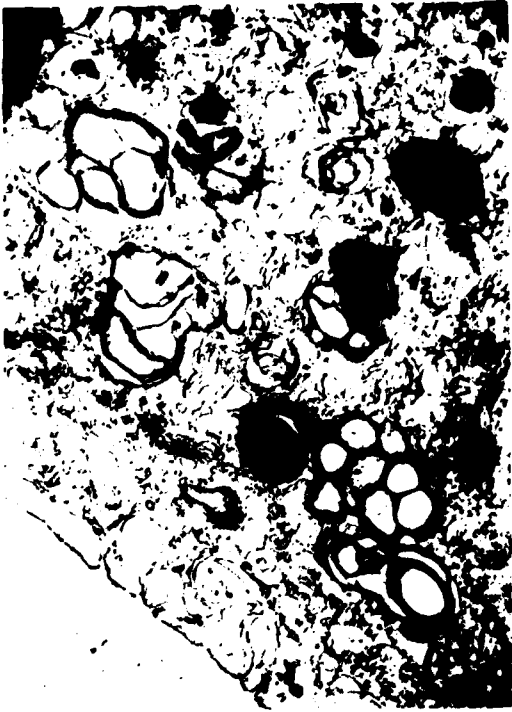
4



46c



47c



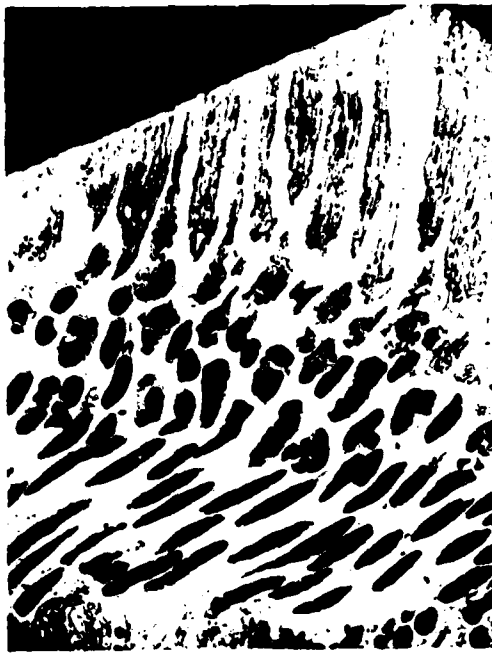
48



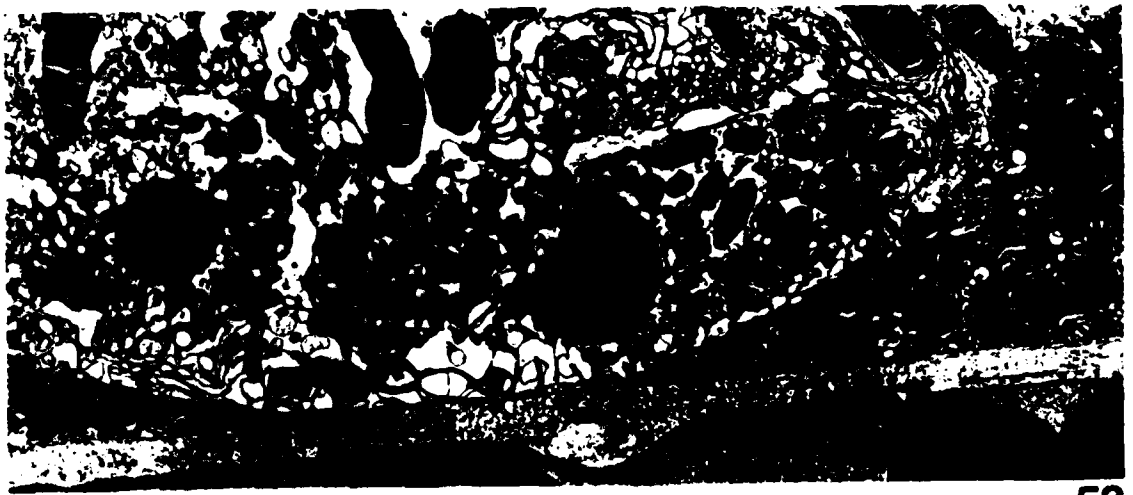
50



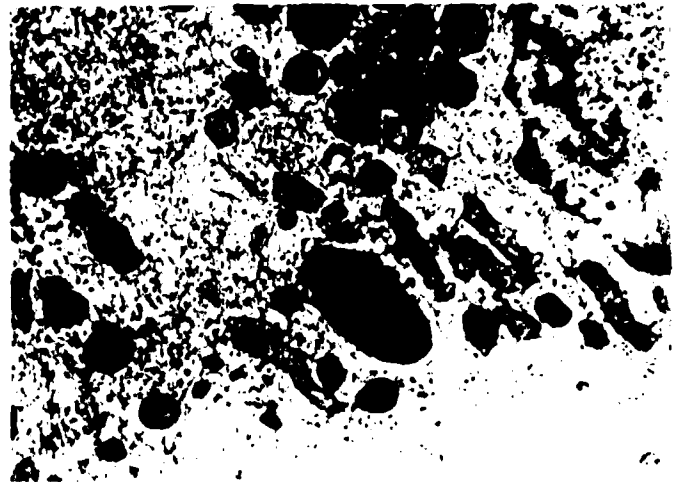
51



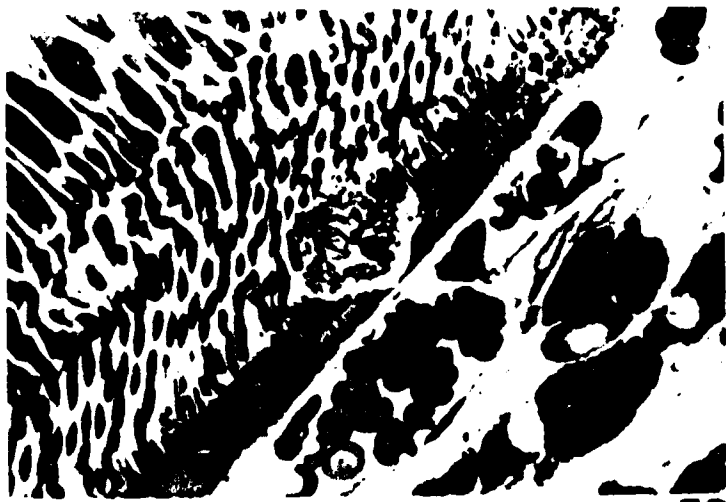
52



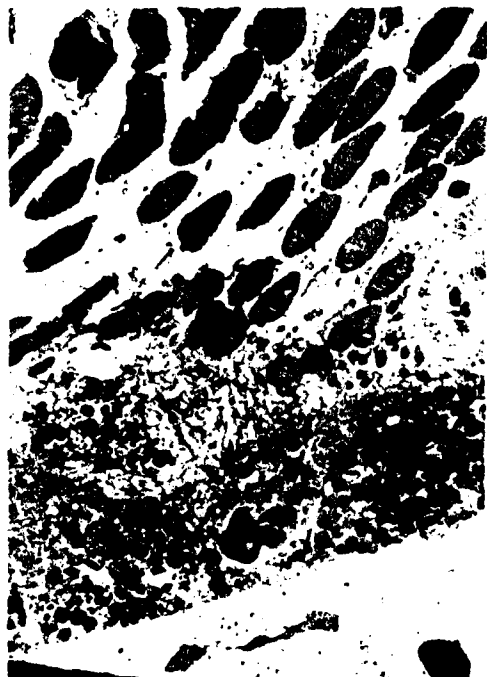
53



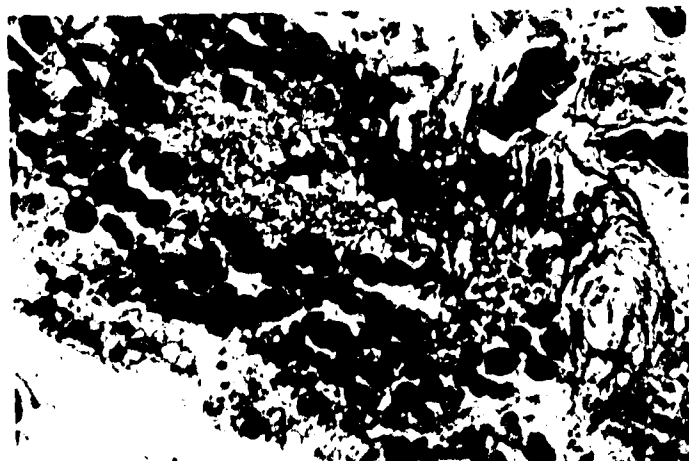
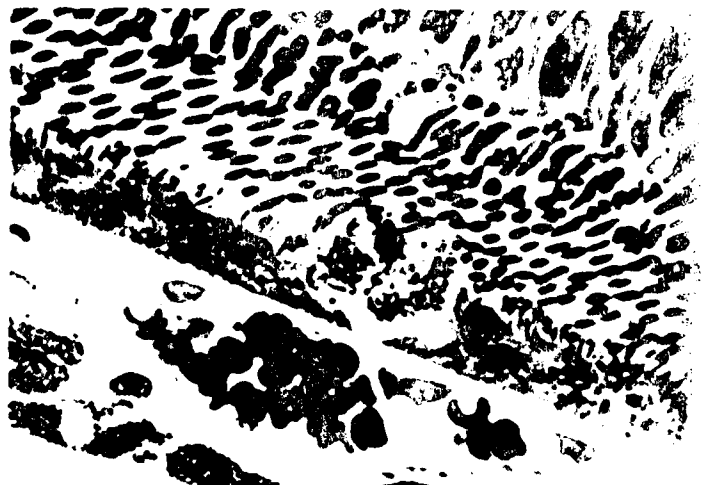
55

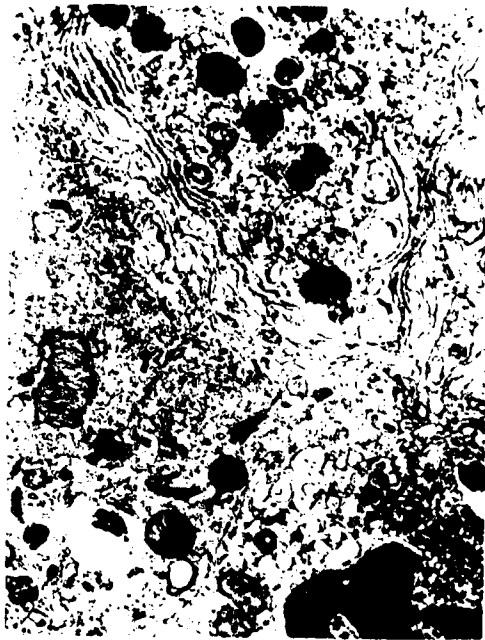


56



58

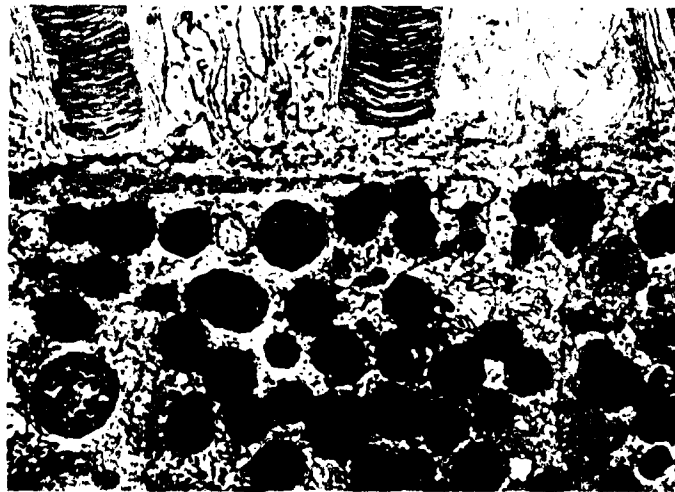




62



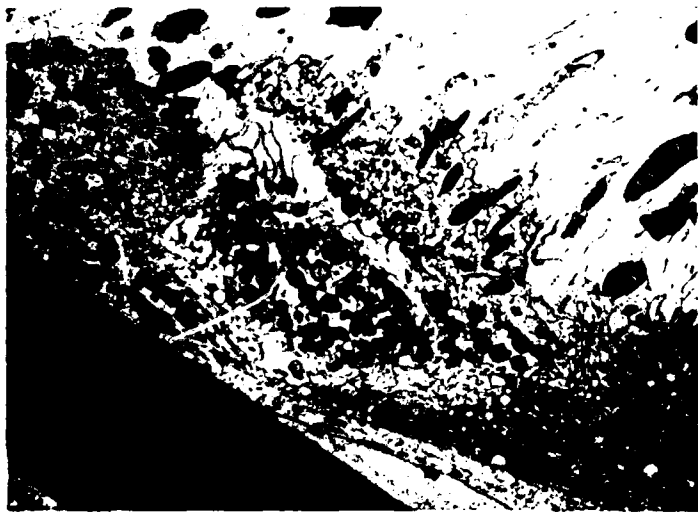
63



64c



65c



66



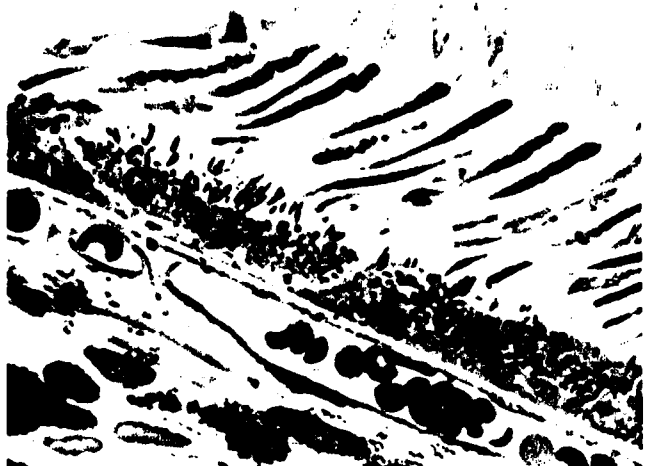
6



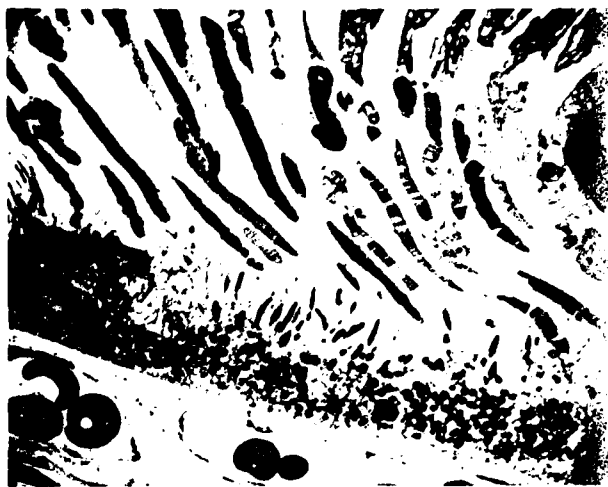
68



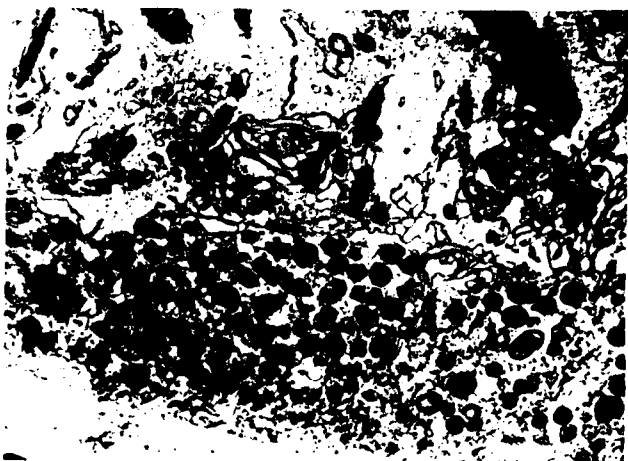
9



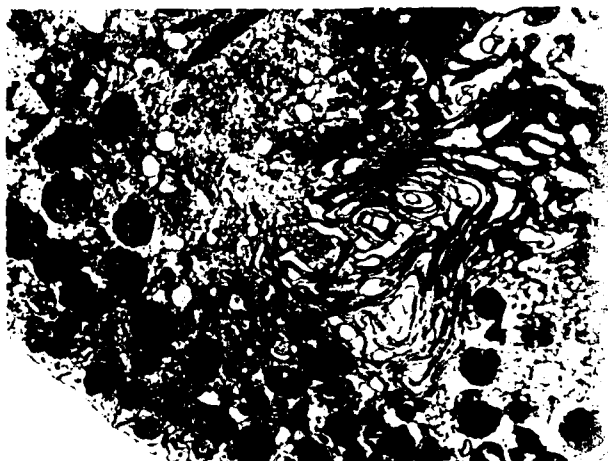
70



71



72



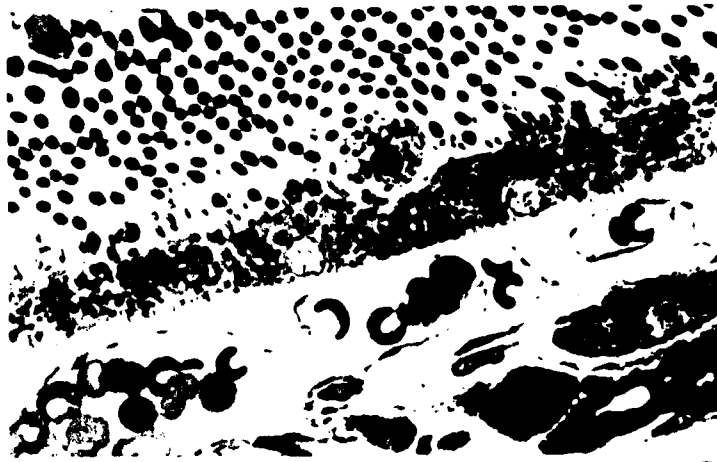
73



74a



75c



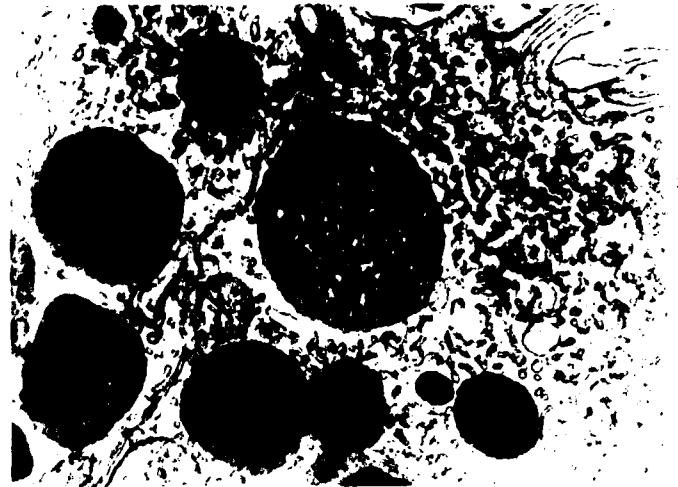
76



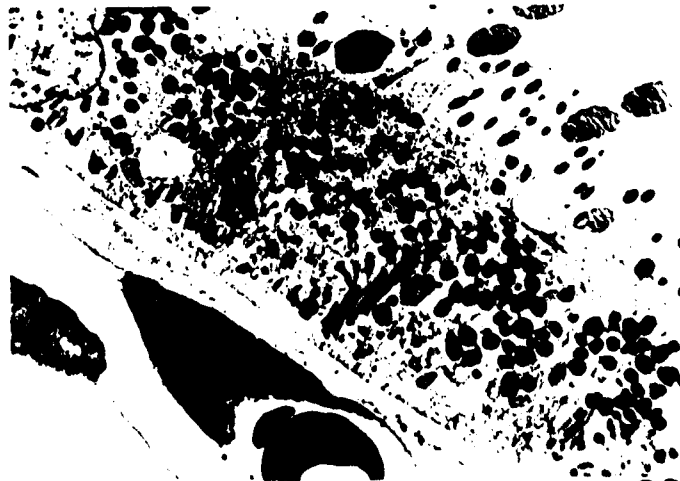
77



78



79



80c

## ACRONYMS AND ABBREVIATIONS

- ~ - approximately
- aq - aqueous
- c - control/s
- D - dextral (right)
- ED<sub>50</sub> - threshold level for production of a laser lesion  
ophthalmoscopically visible 5 minutes after irradiation
- EL - experimental lesion/s
- Fig - figure
- HeNe - Helium neon
- Hz - Hertz (frequency)
- IS - inner segment/s
- I.V. - intravenous
- K Hz - kilohertz
- LAIR - Letterman Army Institute of Research, San Francisco
- LM - light microscopy/micrograph/s
- MB - marker burn
- MG - melanin granule/melanosome
- Mg - milligrams
- ml - millilitres
- μm - micrometre ( $10^{-6}$  metre)
- Mv - microvillus/microvilli
- Nd - neodymium
- nm - nanometres ( $10^{-9}$ m)
- nsec - nanoseconds ( $10^{-9}$ sec)
- OLM - outer limiting membrane
- ONL - outer nuclear layer

- OPL - outer plexiform layer
- OS - outer segment
- $\text{OsO}_4$  - osmium tetroxide
- PE - pigment epithelium
- PR - photoreceptor/s
- RPE - retinal pigment epithelium
- S - sinistral (left)
- SER - smooth endoplasmic reticulum
- ST - synaptic terminals
- TEM - transmission electron microscopy/micrograph/s
- UWO - The University of Western Ontario
- WBC - white blood cell

## REFERENCES

- Adams, D.O., Lund, D.J. and Schawaluk, P.D. The nature of chorioretinal lesions produced by the gallium arsenide laser. *Invest. Ophthalmol.* 13 : 471 -475, 1974.
- Beatrice, E.S., Lund, D.J., Carter, M. and Talsma, D.M. Retinal alterations produced by low level gallium arsenide laser exposure. LAIR Report No. 38, Feb. 1977.
- Kuwabara, T. and Okisaka, S. Effect of electronic strobe flashlight on the monkey retina. *Jap. J. Ophthalmol.* 20 : 9 - 18, 1976.
- Kuwabara, T. Photic photo-thermal effects on the retinal pigment epithelium In: *The retinal pigment epithelium*. Eds. K.M. Zinn and M.F. Marmor, Harvard Univ. Press, pp 293 - 313, 1979
- Lund, D.J., Stuck, B.E. and Beatrice, E.S. Biological research in support of project MILES. LAIR Report No. 96, July 1981.
- Marshall, J., Grindle, J., Ansell, P.L. and Borwein, B. Convolution in human rods : an ageing process. *Brit. J. Ophthalmol.* 63 : 181 - 187, 1979.
- Schuscheereba, S., Zwick, H., Stuck, B.E. and Beatrice, E.S. Macular (foveal) RPE differences after low level exposure to diffuse argon laser radiation-ARVO supplement to *Invest. Ophthalmol. Visual Sci.* 20 : (3) : p. 80, 1981.
- Zinn, K.M. and Benjamin-Henkind, J.V. Anatomy of the human retinal pigment epithelium. In : *The retinal pigment epithelium*. Eds. K. M. Zinn and M.F. Marmor. Harvard Univ. Press, pp. 3 - 31, 1979.

PUBLICATIONS:

1. B. Borwein, M.L. Coetsee and S. Krupko. Development of the embryo-sac of Restio Doodii and Elegia racemosa. (Quoted by Maheshwari, P. The Embryology of Angiosperms, McGraw-Hill, 1950). J. South African Botany, 15: 1-11. 1949.
- P 2. B. Borwein and M. J. Hollenberg. The photoreceptors of the "four-eyed" fish, Anableps anableps L. J. Morph. 140: 405-442. 1973.
- P 3. B. Borwein and M. J. Hollenberg. Mitochondrial origin of the oil droplets in cone photoreceptors of the four-eyed fish Anableps anableps. Proc. Can. Fed. Biol. Soc. 16: 34, 1973.
- \*4. J. Medeiros, B. Borwein, M.J. Hollenberg and J. Wm. McGowan. Effects of suprathreshold laser exposures on the vitreoretinal junction, In: Proc. of the World Health Organization meeting on Health Hazards of Optical Radiation. Dublin, Ireland. 1974.
- P \*5. B. Borwein, M. Sanwal, J.A. Medeiros and J. Wm. McGowan. Scanning electron microscopy of normal and lased rabbit retina. Can. J. Ophthal. 11(4): 309-322. 1976.
- P \*6. B. Borwein, J.A. Medeiros and J. Wm. McGowan. Fusing rod outer segments from an eye enucleated for choroidal melanoma. Invest. Ophthal. and Vis. Sci. 16(7): 678-683. 1977.
- P \*7. B. Borwein, M. Sanwal, J. A. Medeiros and J. Wm. McGowan. Scanning electron microscopy of normal and lased rabbit pigment epithelium. Invest. Ophthal. and Vis. Sci. 16(8): 700-710. 1977.
- \*8. J.A. Medeiros, B. Borwein and J. Wm. McGowan. Spectroscopic characteristics of small dielectric cones. J. Opt. Soc. Am. 67: 1372. 1977. (abstract)
- \*9. J. Marshall, J. Grindle, P. Ansell and B. Borwein. Convolution in human rods: an aging process. British J. of Ophthalmol. 63(3): 181-187. March, 1979.
- \*10. J. Wm. McGowan, B. Borwein, J.A. Medeiros, E. Spiller, R. Feder, J. Topalian and W. Gudat. High resolution microchemical analysis using soft X-ray lithographic techniques. J. Cell Biol. 80: 732-735. 1979.
- \*11. J. A. Medeiros, B. Borwein and J. Wm. McGowan. Application of optical transform techniques to laser irradiation of retina. Investig. Ophthalmol. and Vis. Sci. 18: 602-613. 1979.

- P \*12. B. Borwein, D. Borwein, J. Medeiros and J. Wm. McGowan. Shape, dimensions, and structure of foveal cones of M. mulatta and M. irus. ARVO, Supplement to Investig. Ophthalmol. and Vis. Sci., p. 79, April 1979. (abstract)
- P \*13. B. Borwein, D. Borwein, J. Medeiros and J. Wm. McGowan. The ultrastructure of monkey foveal photoreceptors, with special reference to the structure, shape, size, and spacing of the foveal cones. Amer. J. Anat. 159: 125-146. 1980.
- P \*14. B. Borwein. The Retinal Receptor: A description. Chap. 2. In: Vertebrate Photoreceptor Optics. Springer Series in Optical Sciences, Vol. 23. Springer-Verlag, Berlin, Heidelberg, New York. Eds. J. M. Enoch, F. L. Tobey. pp. 11-81. 1981.
- P \*15. B. Borwein. Scanning electron microscopy of monkey photoreceptors. Can. Fed. Biol. Socs., Montreal. Abstract #546, p. 237. June, 1981.
- P \*16. B. Borwein. Low level (subthreshold) large spot laser irradiations of the retinas of Macaca mulatta. Report to U.S. Army Medical Research Development Command. 56 figs., Dec.1981.
- P \*17. B. Borwein. Neodymium laser lesions in rhesus monkey retina. ARVO, Supplement to Investig. Ophthalmol. and Vis. Sci., p. 52, May 1982.
- P \*18. B. Borwein. Scanning electron microscopy of monkey foveal photoreceptors. Submitted to Anat. Rec. 1982. (Accepted, subject only to being shortened).
- P \*19. B. Borwein. Neodymium laser lesions in rhesus monkey retinas. In preparation for Health Physics, 1982.

Legend

P = Principal or sole author

\* = Supported by USAMRDC

Personnel supported by the Grant:

1. Dr. Bessie Borwein. B.Sc. Hons (Wits. S.A.) (1st class);  
Ph.D. Anatomy (U.W.O.)

Principal Investigator - Assistant Professor,  
Department of Anatomy,  
The University of Western Ontario.

1. Mr. Stephen Smith B.Sc. (The University of Western Ontario)  
with emphasis on Zoology.

Technician

**END**

**FILMED**

**6-85**

**DTIC**